

Quantitative model for ^{13}C tracing applied to citrate production and secretion of prostate epithelial tissue

Frits H.A. van Heijster¹, Vincent Breukels¹, Arend Heerschap¹

¹Radiology and Nuclear Medicine, Radboud University Medical Center, Nijmegen, The Netherlands

Abstract

Healthy human prostate epithelial cells have the unique ability to produce and secrete large amounts of citrate into the lumen of the prostate. Citrate is a Krebs cycle metabolite produced in the condensation reaction between acetyl-CoA and oxaloacetate in the mitochondria of the cell. With the application of ^{13}C enriched substrates, such as ^{13}C glucose or pyruvate, to prostate cells or tissues, it is possible to identify the contributions of different metabolic pathways to this production and secretion of citrate. In this work we present a quantitative model describing the mitochondrial production and the secretion of citrate by prostatic epithelial cells employing the ^{13}C labeling pattern of secreted citrate as readout. We derived equations for the secretion fraction of citrate and the contribution of pyruvate dehydrogenase complex versus the anaplerotic pyruvate carboxylase pathways in supplying the Krebs cycle with carbons from pyruvate for the production of citrate. These measures are independent of initial ^{13}C -enrichment of the administered supplements and of ^{13}C J-coupling patterns, making this method robust also if SNR is low. We propose the use of readout variables of this model to distinguish between citrate metabolism in healthy and diseased prostate tissue, in particular upon malignant transformation.

Introduction

Healthy prostate epithelial cells have the unique capability of secreting citrate in the ducts or lumen of the prostate.¹, where it can reach levels up to about 180 mM. Citrate accumulation in the prostate is promoted by inhibition of the citrate converting enzyme *m*-aconitase through zinc binding, which is taken up at relatively high levels in epithelial prostate cells.¹⁻³ The characteristic citrate accumulation is lost upon malignancy,⁴ and a decreased citrate signal in MR spectroscopic images of the prostate is used as a biomarker for the presence of cancer.⁵⁻⁷ Prostate cancer accounts for one in five cancers and is responsible for one in ten cancer related deaths in men worldwide.^{8,9} Understanding metabolic reprogramming in malignant transformation may help to better diagnose and treat prostate cancer.¹⁰⁻¹³ Citrate is the product of a condensation reaction of oxaloacetate and acetyl-CoA catalyzed by citrate synthase as the first step of the Krebs cycle. A major compound from which acetyl-CoA is derived is glucose, which is metabolized into pyruvate by glycolysis and subsequently enters the mitochondria where it is converted into acetyl-CoA to enter the Krebs cycle. In this step two carbons enter the cycle, which is equal to the carbon efflux as carbon dioxide, during one Krebs cycle turn. Because of citrate efflux into the luminal space, removing six carbons from the cycle, anaplerotic contributions are required to maintain the carbon pool of the Krebs cycle. One of these anaplerotic contributions can come from pyruvate being converted into oxaloacetate by pyruvate carboxylase (PC). The influx of this four-carbon metabolite can partly balance the efflux of six carbon citrate every Krebs cycle turn.

The carbon flow for citrate production and secretion can be assessed by supplying prostate tissue or cells *in vivo* or *in vitro* with ¹³C substrates and monitoring the fate of the ¹³C-labels by ¹³C MR spectroscopy or high resolution ¹³C NMR spectroscopy and subsequently looking at the specific ¹³C labeling of metabolic products. In this way metabolic routes involved in citrate generation can be delineated and quantified.

Multiple metabolic flux modeling studies have modeled Krebs cycle activity in different tissues and cell types under different conditions. This has been done using (extensive) metabolic networks involving fluxes between the metabolites in the network, like positional isotopomers¹⁴, bonded cumomer analysis¹⁵ or elementary metabolite unit based methods¹⁶. For example, in human melanoma cell line DB1, rat C6 glioma cells, H460 NSCLC cells, hepatocytes and brown adipocytes and in isolated cardiac mitochondria relative fluxes of total TCA cycle activity V_{TCA} and exchange flux V_x of α -ketoglutarate with glutamate V_x have been determined *in vitro*.¹⁷⁻²³ But also *in vivo* in mouse and rat brain and heart²⁴⁻²⁸ and human brain.²⁹⁻³¹ The fast exchange between glutamate and α -ketoglutarate is one common element in these studies. Overall, the different contributions of pyruvate carboxylase activity, malic enzyme activity, glutaminolysis and other cataplerotic and anaplerotic processes³² for different tissues and cells make it hard to generalize Krebs cycle metabolism in such a way that it can be used to predict prostate metabolism. Moreover, the unique features of citrate metabolism in the prostate make it hard to translate values found in these other studies to prostate metabolism. Most NMR investigations with ¹³C labeling of prostate tissue have been performed with hyperpolarization of the substrates^{33,34}, but none have been focusing on citrate metabolism.

The unique characteristic secretion of citrate by prostatic cells provides a six-carbon readout of this Krebs cycle activity, which has not been explored before as far as we know. A first practical approach to explore this property would be in studies of prostate cells, but most prostatic epithelial cell lines lack the capacity of citrate secretion. However, the prostate cancer metastasis cell line LNCaP has been shown to still have the capacity to secrete citrate and therefore may

serve as a convenient model system to evaluate if ^{13}C labeling of secreted citrate can be explored as a readout for carbon flow inside the cell.³⁵⁻³⁷ Using only simple ratios of the presence of ^{13}C in citrate, which can be extracted from MR spectroscopic data or high resolution ^{13}C NMR spectra, we developed a simple quantitative model for cellular citrate production in this work. On one hand we determine an index for citrate production and secretion versus Krebs cycle consumption and on the other hand an estimate of the balance between pyruvate carboxylase (PC) and pyruvate dehydrogenase complex (PDC) activity in citrate production.

Scope of data suitable for the model

To follow citrate metabolism in healthy or malignant prostate epithelial tissue *in vivo*, or *in vitro* in primary cell cultures or cell lines, various ^{13}C labeled substrates can be used. Although in principle we could model the metabolic pathways for any of these, for the purpose described above, we specifically focused on the application of $[1,6-^{13}\text{C}_2]$ glucose or $[3-^{13}\text{C}]$ pyruvate (both substrates result in the same citrate labeling pattern, as shown below) and on $[2,5-^{13}\text{C}_2]$ glucose or $[2-^{13}\text{C}]$ pyruvate (also both resulting in the same citrate labeling pattern). In practice, these substrates can be administered long enough to the cells (e.g. 48h) to reach a steady state of ^{13}C labeling of citrate secreted in the extracellular fluid or incubation medium. Extracellular material can then be collected and analyzed by high resolution ^{13}C (and ^1H) NMR spectroscopy. Citrate resonances can be identified and quantified (e.g. using *j*MRUI AMARES³⁸⁻⁴⁰) for further use, e.g as input in the model. Using $[3,4-^{13}\text{C}_2]$ glucose or $[1-^{13}\text{C}]$ pyruvate would not result in labeling of citrate via the PDC pathway, but only via the PC pathway.

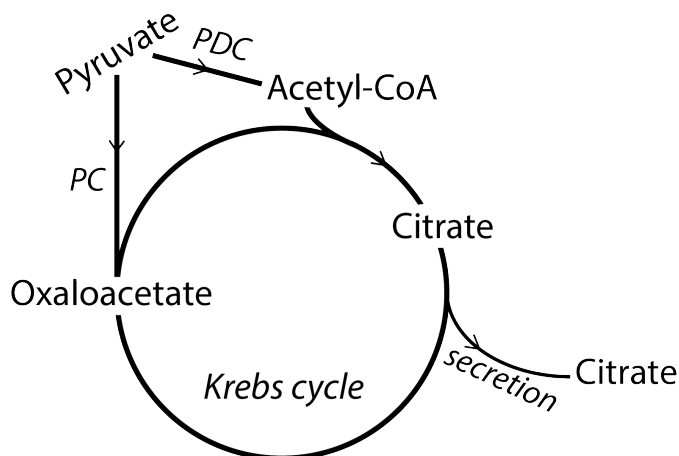


Figure 1: Schematic overview of the basic elements of the quantitative model for citrate secretion. Pyruvate can contribute carbons to the Krebs cycle either as Acetyl-CoA, through pyruvate dehydrogenase complex route (PDC), or in oxaloacetate, via the pyruvate carboxylase route (PC). Oxaloacetate and acetyl-CoA undergo a condensation reaction providing citrate, which is partially secreted. Note that this figure shows only the basics of our model and that other contributions to these pathways (anaplerotic and cataplerotic) are considered (see text).

Quantitative model

The distribution of ^{13}C carbons in citrate, as determined from NMR spectra, reflects on the ratio of pyruvate going into the Krebs cycle via pyruvate carboxylase (as oxaloacetate) and pyruvate dehydrogenase (as acetyl-CoA) on one hand and on the fraction of molecules leaving the Krebs cycle, in every turn of this cycle, to be secreted into the lumen or incubation medium on the other hand (Figure 1). Here we derive a quantitative model describing prostatic citrate production depending on a (constant) secretion fraction c and on the fractions of carbons (either ^{13}C labeled or unlabeled) entering via acetyl-CoA (f^{PDC}) or oxaloacetate (f^{PC}), with $f^{PC} + f^{PDC} = 1$. The ^{13}C labeling at the six different positions in citrate secreted and carbon dioxide produced at cycle turn n is described by $\vec{C}(n)$.

$$\vec{C}(n) = \begin{pmatrix} C_1(n) \\ C_2(n) \\ C_3(n) \\ C_4(n) \\ C_5(n) \\ C_6(n) \\ CO_2(n) \end{pmatrix} c(1-c)^n \quad (1)$$

Since every Krebs cycle turn a fraction c of citrate leaves the cycle and fraction $(1-c)$ remains in the cycle a factor $c(1-c)^n$ is included. For example, if at $n=3$ citrate molecules are secreted with 20% label on C_2 , 10% on C_4 and 5% on C_5 and C_6 , and 3% label is lost in carbon dioxide, this would be described by:

$$\vec{C}(n) = \begin{pmatrix} 0 \\ 0.2 \\ 0 \\ 0.1 \\ 0.05 \\ 0.05 \\ 0.03 \end{pmatrix} c(1-c)^3 \quad (2)$$

Equations describing the labeling of each of the six carbons in secreted citrate are derived further on in this paper.

Fate of ^{13}C labels in the Krebs cycle

When a ^{13}C label enters the Krebs cycle it can end up at different positions in citrate (see Figure 2). If a label continues along the Krebs cycle it can eventually end up in citrate again, but now at a different position, or even distributed equally over two citrate carbon positions. This is because succinate and fumarate are symmetrical intermediates in the Krebs cycle resulting in the indistinguishable labeling of C1 and C4 or of C2 and C3 in succinate and fumarate. Eventually this leads to an equal distribution of ^{13}C labels at two carbon positions in citrate. The position of ^{13}C labels at citrate carbons C1-C6 and oxaloacetate (OAA) at cycle turn $n+1$ versus n are shown in Table 1.

$Citr(n)$	\Rightarrow	$OAA(n)$	\Rightarrow	$Citr(n+1)$
$C1$	\Rightarrow	$\frac{1}{2}C1 + \frac{1}{2}C4$	\Rightarrow	$\frac{1}{2}C5 + \frac{1}{2}C6$
$C2$	\Rightarrow	$\frac{1}{2}C2 + \frac{1}{2}C3$	\Rightarrow	$\frac{1}{2}C3 + \frac{1}{2}C4$
$C3$	\Rightarrow	$\frac{1}{2}C2 + \frac{1}{2}C3$	\Rightarrow	$\frac{1}{2}C3 + \frac{1}{2}C4$
$C4$	\Rightarrow	$\frac{1}{2}C1 + \frac{1}{2}C4$	\Rightarrow	$\frac{1}{2}C5 + \frac{1}{2}C6$
$C5$	\Rightarrow	CO_2		
$C6$	\Rightarrow	CO_2		

Table 1: Shifting of carbons of citrate during the Krebs cycle. Shown are citrate (Citr) at Krebs cycle turn n , oxaloacetate (OAA) at cycle turn n and citrate at cycle turn $n+1$. Cycle turn n starts at the secretion of citrate and ends upon formation of new citrate in the subsequent cycle turn.

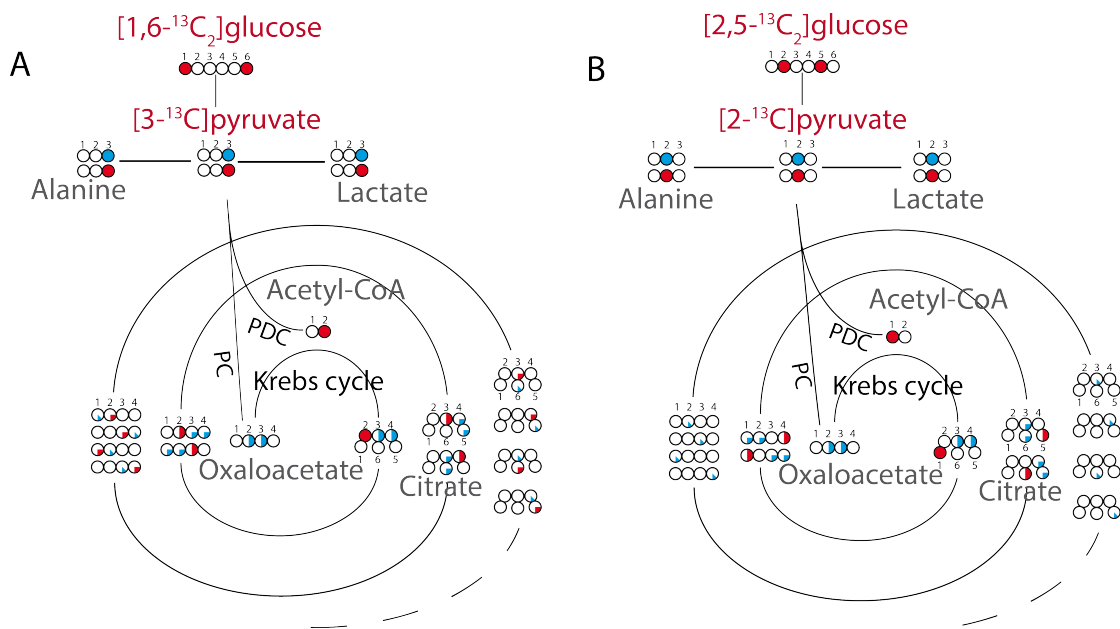


Figure 2: Schematic representation of the fate of ^{13}C carbons entering the Krebs cycle during subsequent cycle turns. A.) The distribution of ^{13}C labels originating from $[1,6-^{13}C_2]$ glucose or $[3-^{13}C]$ pyruvate. (B) Idem for $[2,5-^{13}C_2]$ glucose or $[2-^{13}C]$ pyruvate. Pyruvate carbons converted to oxaloacetate by pyruvate carboxylase (PC) are indicated by blue circles and those converted into acetyl-CoA by pyruvate dehydrogenase complex (PDC) by red circles. Rapid exchange between oxaloacetate and fumarate equally distributes the labeling of oxaloacetate via PC over the two middle carbons. In this figure the carbon numbers in each compound are indicated and for simplicity mitochondrial and cellular export of citrate is omitted. In this figure no new ^{13}C label is flowing into the Krebs cycle during the subsequent cycle turns, this however is taken into account in the sections below.

First labeling of citrate ($n = 0$)

The (^{13}C) carbons of pyruvate can enter the Krebs cycle via the pyruvate carboxylase (PC) and the pyruvate dehydrogenase complex (PDC) route. We define Krebs cycle turn n as the number of full Krebs cycle turns completed before secretion of citrate from the Krebs cycle. This means that if citrate is secreted right after it is labeled, this is Krebs cycle turn $n = 0$. This is the only cycle turn where ^{13}C carbons enter the Krebs cycle via PC because the oxaloacetate during the next Krebs cycle turns ($n > 0$) originates from the citrate in the previous Krebs cycle turn that is not secreted. On the other hand, this oxaloacetate undergoes a condensation reaction with a ^{13}C labeled acetyl-CoA forming citrate every Krebs cycle turn, so carbons enter the Krebs cycle via PDC every cycle turn. The first labeled citrate (at $n = 0$) can have a different label depending on the labeling of pyruvate (or acetyl-CoA). For $[1,6-^{13}\text{C}_2]$ glucose or $[3-^{13}\text{C}]$ pyruvate the route of labeling of citrate is shown in Figures 2 and 3. The ^{13}C labeled oxaloacetate (OAA) and ^{13}C labeled acetyl-CoA can, together with unlabeled oxaloacetate or acetyl-CoA, undergo a condensation reaction to produce unlabeled, single- or double ^{13}C labeled citrate. This results in citrate labeled at C2 (PDC) and/or C1/4 (PC) respectively at $n = 0$. The labeling of oxaloacetate is distributed over two carbons due to rapid exchange between oxaloacetate, malate and (symmetrical) fumarate.^{41,42} If $[2,5-^{13}\text{C}_2]$ glucose or $[2-^{13}\text{C}]$ pyruvate are applied as substrate the labeling paths as shown in Figure 2B (or Figure 4) are followed, resulting in citrate labeling at C1 (PDC) and/or C2/3 (PC) respectively at $n = 0$.

Note here that if P and A were to be the fractions of ^{13}C label ending up in oxaloacetate via PC or in acetyl-CoA via PDC respectively, the resulting distribution of ^{13}C label over the three citrate positions that are possibly labeled at $n = 0$ is equal to $\frac{P}{2}$ at two positions and A at the other. For the $[1,6-^{13}\text{C}_2]$ glucose or $[3-^{13}\text{C}]$ pyruvate experiment this would be A label at C2 and P labels distributed over C3 and C4. For the ^{13}C $[2,5-^{13}\text{C}_2]$ glucose or $[2-^{13}\text{C}]$ pyruvate experiment this results in A label at the C1 position and P label distributed over the C3 and C4 position.

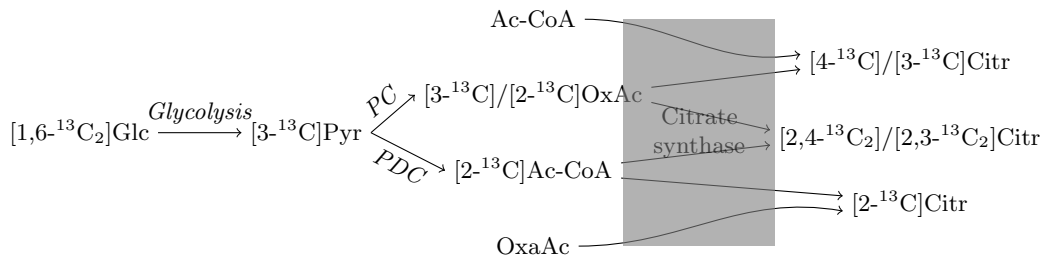


Figure 3: For $n = 0$ the ^{13}C labels originating from $[1,6-^{13}\text{C}_2]$ glucose or $[3-^{13}\text{C}]$ pyruvate end up in oxaloacetate (at C2 or C3) via pyruvate carboxylase or in acetyl-CoA (at C2) via pyruvate dehydrogenase complex before ending up in citrate after the condensation reaction of acetyl-CoA and oxaloacetate. This can result in unlabeled (not shown), single labeled and double labeled citrate. Glc = glucose, Pyr = pyruvate, Ac-CoA = acetyl-CoA, OxAc = oxaloacetate.

Pyruvate carboxylase versus pyruvate dehydrogenase complex

To determine the fractional contributions of the PC and PDC routes to the final citrate pool in the luminal fluid or incubation medium it is essential to realize that depending on how many Krebs cycle turns a ^{13}C label completes before being secreted, the contribution is different. Let's start with fraction A ^{13}C labels getting into citrate via PDC and fraction P ^{13}C labels getting

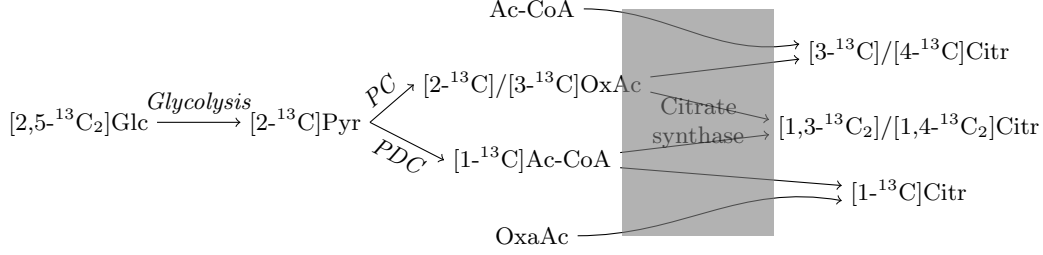


Figure 4: For $n = 0$ the ^{13}C labels originating from $[2,5-^{13}\text{C}_2]$ glucose or $[2-^{13}\text{C}]$ pyruvate can either end up in oxaloacetate (at C2 or C3) via pyruvate carboxylase or in acetyl-CoA (at C1) via pyruvate dehydrogenase complex before it ends up in citrate after the condensation reaction of acetyl-CoA and oxaloacetate. This can result in unlabeled (not shown), single labeled and double labeled citrate. Glc = glucose, Pyr = pyruvate, Ac-CoA = acetyl-CoA, OxAc = oxaloacetate.

into citrate via PC. Subsequently fraction c of the citrate will be secreted (we have defined this as Krebs cycle turn $n = 0$) and fraction $(1 - c)$ continues in the Krebs cycle. Now $(1 - c)$ carbon skeletons will be labeled again upon condensation of the carbon skeleton (oxaloacetate) with $(1 - c)$ ^{13}C acetyl-CoA forming $(1 - c)$ citrate. Of this citrate again fraction c is secreted (at cycle turn $n = 1$) and fraction $(1 - c)$ continues down the Krebs cycle and the process repeats itself. This is summarized in Figure 5. Pyruvate carboxylase only contributes to the ^{13}C labeling of the citrate pool in the luminal fluid or incubation medium at $n = 0$ and pyruvate dehydrogenase complex contributes to the citrate pool during all Krebs cycle turns. In general, during cycle turn $n > 0$ there will be $A(1 - c)^n$ labels entering the cycle and $Ac(1 - c)^n$ citrate molecules will be secreted. Only at $n = 0$ there will be $A + P$ labels entering the cycle and $c(A + P)$ citrate molecules will be secreted. The sum of all fractions of ^{13}C labels entering the Krebs cycle has to be equal to $f^{PC} + f^{PDC} = 1$ and since the only time labels originating from the PC route can enter the cycle is at turn $n = 0$, we can easily see that the fraction f^{PC} of pyruvate carbons is equal to the fraction P of ^{13}C pyruvate carbons described above. As fraction f^{PDC} has to be equal to the sum of fractions of ^{13}C labels entering via acetyl-CoA, this comes down to the following sum:

$$f^{PDC} = A \sum_{n=0}^{n=\infty} (1 - c)^n = \frac{A}{c} \quad (3)$$

This means that if at $n = 0$ the fraction f^{PC} of pyruvate ^{13}C labels enter the cycle via the PC route and fraction $A = cf^{PDC}$ enters the cycle via the PDC route, summed over all possible Krebs cycle turns a total of $f^{PC} + \frac{cf^{PDC}}{c} = f^{PC} + f^{PDC} = 1$ ^{13}C of the labels enter the Krebs cycle (Figure 6).

Average number of completed Krebs cycle turns before citrate secretion

The average number of Krebs cycle turns before secretion of citrate (This is not the same as the average number of Krebs cycle turns a ^{13}C carbon completes, see Appendices for the average number of cycle turns a ^{13}C carbon completes) depends on the secretion fraction c . To calculate this average number of cycle turns $\langle n \rangle$ the sum can be calculated of the fractions secreted

every cycle $c(1 - c)^n$ multiplied with their corresponding Krebs cycle turn indices n .

$$\langle n \rangle = c \sum_{n=0}^{n=\infty} n(1 - c)^n = \frac{1 - c}{c} \quad (4)$$

The average number of cycle turns is equal to the ratio of the fraction of molecules that stay in the Krebs cycle $(1 - c)$ over the fraction of molecules that are secreted c .

Effect of ^{13}C enrichment

Until now, we assumed that all pyruvate or glucose carbons are ^{13}C labeled and that both the pyruvate pool and acetyl-CoA pool are fully labeled. This probably doesn't reflect the true situation in cells or tissue because of influx of unlabeled pyruvate (e.g. via Malic Enzyme or PEPCK) or acetyl-CoA (e.g. via beta oxidation). To take this into account, introducing enrichment factors in the equations is needed. Suppose only fraction ϵ_p of pyruvate and fraction ϵ_a of acetyl-CoA is ^{13}C labeled, then fractions $\epsilon_p\epsilon_a c f^{PDC}$ (via pyruvate dehydrogenase complex) and $\epsilon_p f^{PC}$ (via pyruvate carboxylase) of ^{13}C carbons will enter the Krebs cycle at $n = 0$, $\epsilon_p\epsilon_a c f^{PDC}(1 - c)$ at $n = 1$, $\epsilon_p\epsilon_a c f^{PDC}(1 - c)^2$ at $n = 2$ and so forth. This means that the contributions of the individual cycle turns to the sum (final ^{13}C distribution over citrate carbons) are all multiplied by ϵ_p , but only the carbons going via the PDC route (involving acetyl-CoA) are also multiplied with ϵ_a . This only holds if the values of ϵ_p and ϵ_a are not time-dependent. If high enough concentrations or constant inflow of ^{13}C substrate is provided, we can safely assume this to be true during most of the infusion or incubation period. For sake of simplicity we will first derive equations for the ^{13}C distribution of citrate assuming both enrichment fractions to be 1, and later reintroduce these fractions.

Assumptions made in deriving the quantitative model

In deriving this model we assumed firstly that ^{13}C carbons of pyruvate can only enter the Krebs cycle via the pyruvate carboxylase (PC) route, resulting in labeled oxaloacetate or via the pyruvate dehydrogenase complex (PDC) route, resulting in labeled acetyl-CoA. Other pathways are assumed to be negligible. Secondly we assume that a dominant part of molecules leaving the Krebs cycle is due to citrate secretion, and therefore we later define the total fraction of citrate and other molecules (citrate equivalents) to be an apparent citrate secretion fraction d . If there are no other cataplerotic pathways involved, this fraction d is equal to the true citrate secretion fraction c . This is assumed during the derivation of the equations below, but fraction d is reintroduced afterwards for completeness. Thirdly, we assume that the ^{13}C -enrichments of both the pyruvate and acetyl-CoA pool are constant over time. Deriving the equations below we assume both to be 1, but take them into account later. We also assume that ^{13}C -labeled citrate or citrate equivalents (Krebs cycle metabolites) diverged from the Krebs cycle only to reenter the Krebs cycle through exchange, and not at a different position in the Krebs cycle after being converted into another Krebs cycle metabolite, so no short-cuts within the Krebs cycle. The effect of these short-cuts is assumed to be negligible and therefore ignored in this manuscript. We also assume that the fraction of carbon skeletons diverging from the Krebs cycle every cycle turn remains constant over the time period of the experiments. If labeled citrate is used for lipid synthesis, this can result in backflow of labels into the Krebs cycle via oxaloacetate, this effect is expected to be negligible and is therefore not taken into account.

Important to note is: Anaplerotic inflow of (unlabeled) carbons from e.g. glutamine, aspartate or malate during supplementation with $[1,6-^{13}\text{C}_2]$ glucose or $[2-^{13}\text{C}]$ pyruvate do not contribute

to the ^{13}C -labeling pattern of citrate since they do not contribute (see assumption below) ^{13}C -carbons to either the ^{13}C pools of pyruvate or acetyl-CoA. Next to this, exchange of Krebs cycle metabolites with metabolites outside the Krebs cycle does not change the labeling pattern of the citrate that is secreted, but do lead to loss of citrate equivalents. For example, exchange of oxaloacetate with a potential aspartate pool or the exchange of α -ketoglutarate with the glutamate pool does not change the labeling pattern of the α -ketoglutarate that continues in the Krebs cycle. Even if it continues to be converted to glutamine and back. It does however lead to loss of carbon skeletons (citrate equivalents) if there's net flux of α -ketoglutarate to the glutamate pool. These cataplerotic pathways are thus contributing to the apparent citrate secretion fraction d and this apparent citrate secretion fraction is thus an overestimation of the real citrate secretion fraction. Fast exchange between malate, fumarate and oxaloacetate results in full scrambling of the carbons in oxaloacetate produced via the pyruvate carboxylase pathway. And the fast exchange between citrate, isocitrate and α -ketoglutarate results in loss of citrate C6 labeling, taken into account by introducing a dilution factor ϵ_c later on.

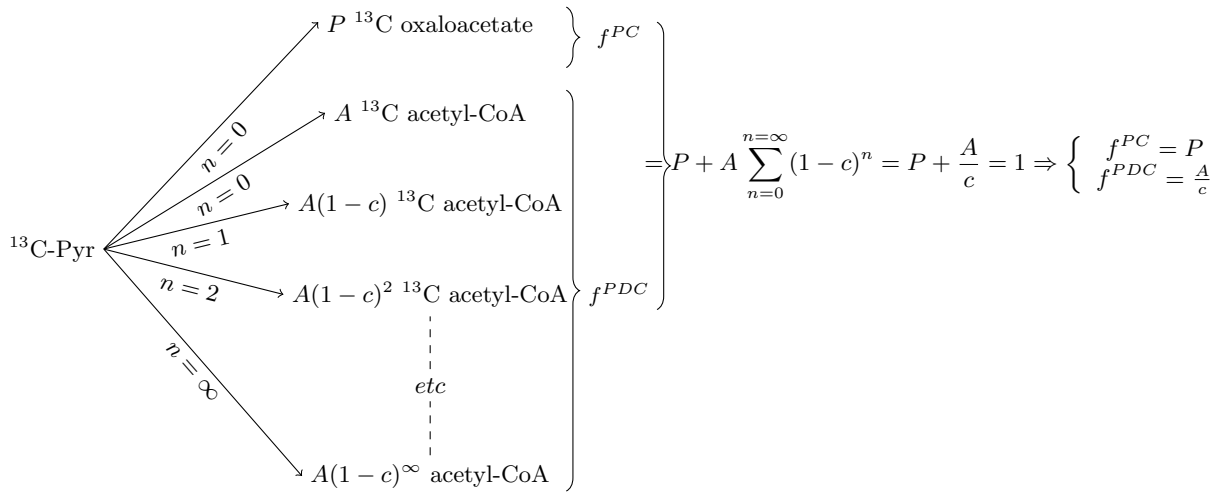


Figure 5: Fate of ^{13}C labels of pyruvate entering the Krebs cycle and ending up in citrate. Fraction $P = f^{PC}$ enters via the pyruvate carboxylase pathway as oxaloacetate (only at $n = 0$), fraction $f^{PDC} = \frac{A}{c}$ flows into the Krebs cycle via the pyruvate dehydrogenase complex pathway as acetyl-CoA.

Providing [1,6- $^{13}\text{C}_2$]glucose or [3- ^{13}C]pyruvate to tissue/cells

To analyze how glucose or pyruvate contribute to the production and secretion of citrate, [1,6- $^{13}\text{C}_2$]glucose or [3- ^{13}C]pyruvate can be provided to epithelial cells or tissue for a longer period of time. Glucose is taken up by the cells and converted into pyruvate during glycolysis. In case of [1,6- $^{13}\text{C}_2$]glucose the ^{13}C label will be located at the C3 position of pyruvate as shown in section "First labeling of citrate ($n = 0$)". Subsequently this label can end up at the oxaloacetate C2 and C3 position, or acetyl-CoA C2 position. The first will result in labeling at C3 or C4 of citrate, the latter at C2. So, the ^{13}C carbon distribution in citrate at cycle turn $n = 0$ will look

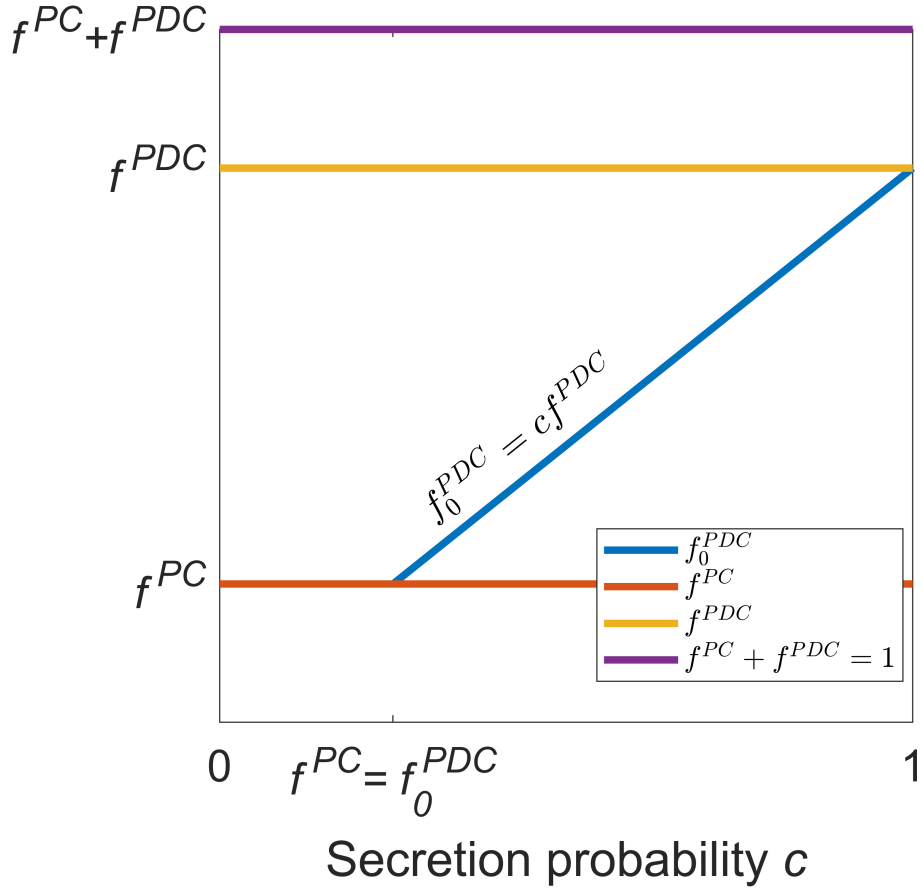


Figure 6: Fractions of carbons diverging via pyruvate carboxylase f^{PC} and via pyruvate dehydrogenase complex f^{PDC} versus secretion fraction c . The sum of f^{PC} and f^{PDC} is equal to 1. The initial fraction (at $n = 0$) of carbons entering the Krebs cycle via PDC (f_0^{PDC}), depends on the value of c , since $f^{PDC} = f_0^{PDC} \sum_{n=0}^{\infty} (1-c)^n = \frac{f_0^{PDC}}{c}$. Next to this, $f_0^{PDC} \leq f^{PC}$, since for every oxaloacetate labeled via the PC route, there is an acetyl-CoA needed (labeled by PDC) at $n = 0$, making the blue line start at $f^{PC} = c f^{PDC}$

like (neglecting carbon dioxide for now):

$$\vec{C}(n=0) = \begin{pmatrix} 0 \\ c f^{PDC} \\ \frac{1}{2} f^{PC} \\ \frac{1}{2} f^{PC} \\ 0 \\ 0 \end{pmatrix} c \quad (5)$$

After one turn the distribution will have shifted according to Table 1 and a new label is entered at the C2 position via PDC.

$$\vec{C}(n=1) = \begin{pmatrix} 0 \\ cf^{PDC} \\ \frac{c}{2}f^{PDC} + \frac{1}{4}f^{PC} \\ \frac{c}{2}f^{PDC} + \frac{1}{4}f^{PC} \\ \frac{1}{4}f^{PC} \\ \frac{1}{4}f^{PC} \end{pmatrix} c(1-c) \quad (6)$$

We assume here that all the label entering at the C2 position is ^{13}C enriched as discussed in section "Effect of ^{13}C enrichment". For cycle turns $n \geq 2$ the distribution at cycle n can be written in a more general way as:

$$\vec{C}(n \geq 2) = \begin{pmatrix} 0 \\ cf^{PDC} \\ \sum_{i=1}^{i=n} \frac{(1-c)^n}{2^i} cf^{PDC} + \frac{(1-c)^n}{2^{n+1}} f^{PC} \\ \sum_{i=1}^{i=n} \frac{(1-c)^n}{2^i} cf^{PDC} + \frac{(1-c)^n}{2^{n+1}} f^{PC} \\ \sum_{i=1}^{i=n} \frac{(1-c)^n}{2^i} cf^{PDC} + \frac{(1-c)^n}{2^{n+1}} f^{PC} \\ \sum_{i=2}^{i=n} \frac{(1-c)^n}{2^i} cf^{PDC} + \frac{(1-c)^n}{2^{n+1}} f^{PC} \end{pmatrix} c \quad (7)$$

We would like to know the distribution of ^{13}C labels over the six citrate carbons in the extracellular fluid or incubation medium when the citrate ^{13}C distribution is in a steady state. This distribution can be calculated by summing the contributions of citrate secreted during each individual Krebs cycle turn n to the total secreted citrate:

$$\vec{C}_{distr}^{1,6-glc} = \sum_{n=0}^{n=\infty} \vec{C}(n) = \begin{pmatrix} 0 \\ cf^{PDC} \sum_{j=0}^{j=\infty} (1-c)^j \\ cf^{PDC} \sum_{j=1}^{j=\infty} \sum_{i=1}^{i=j} \frac{(1-c)^j}{2^i} + f^{PC} \sum_{j=0}^{j=\infty} \frac{(1-c)^j}{2^{j+1}} \\ cf^{PDC} \sum_{j=1}^{j=\infty} \sum_{i=1}^{i=j} \frac{(1-c)^j}{2^i} + f^{PC} \sum_{j=0}^{j=\infty} \frac{(1-c)^j}{2^{j+1}} \\ cf^{PDC} \sum_{j=2}^{j=\infty} \sum_{i=2}^{i=j} \frac{(1-c)^j}{2^i} + f^{PC} \sum_{j=0}^{j=\infty} \frac{(1-c)^j}{2^{j+1}} \\ cf^{PDC} \sum_{j=2}^{j=\infty} \sum_{i=2}^{i=j} \frac{(1-c)^j}{2^i} + f^{PC} \sum_{j=0}^{j=\infty} \frac{(1-c)^j}{2^{j+1}} \end{pmatrix} c = \begin{pmatrix} 0 \\ f^{PDC} \\ \frac{1-c}{1+c} f^{PDC} + \frac{1}{1+c} f^{PC} \\ \frac{1-c}{1+c} f^{PDC} + \frac{1}{1+c} f^{PC} \\ \frac{1-c}{2(1+c)} ((1-c)f^{PDC} + f^{PC}) \\ \frac{1-c}{2(1+c)} ((1-c)f^{PDC} + f^{PC}) \end{pmatrix} c \quad (8)$$

These equations give the ^{13}C label distribution over the six carbons in secreted citrate. This distribution only depends on c and the fraction of carbon entering the Krebs cycle via the

pyruvate carboxylase route, f^{PC} , since $f^{PDC} = 1 - f^{PC}$. The ^{13}C distribution for $f^{PC} = 0.2$ is plotted against c in figure 7, the distribution of ^{13}C labels over the six citrate carbons (and the fraction ending up in CO_2) is strongly dependent on secretion fraction c . The distribution over the different carbons serves as a fingerprint for secretion fraction c .

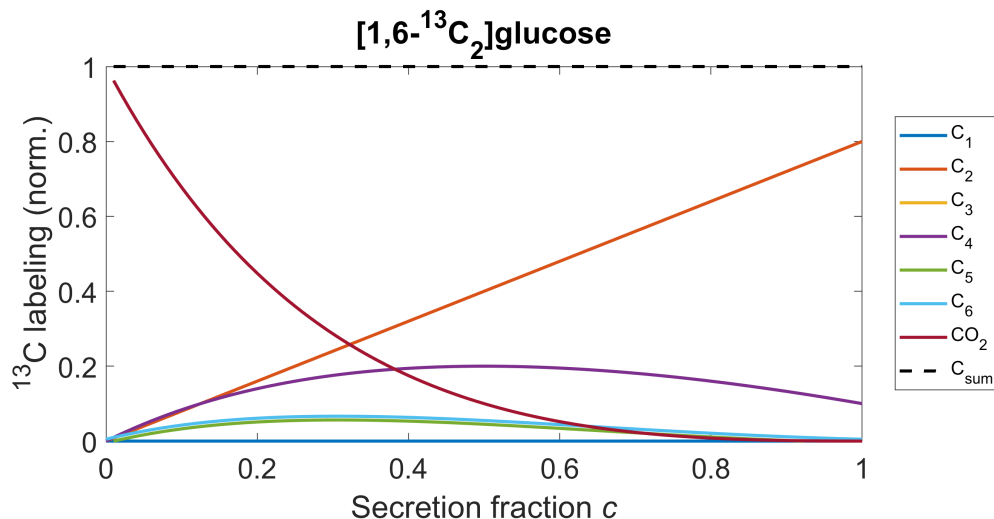


Figure 7: ^{13}C distribution over the six citrate carbons versus secretion fraction c after providing $[1,6-^{13}\text{C}_2]\text{glucose}$ or $[3-^{13}\text{C}]\text{pyruvate}$ to prostate epithelial tissue or cells. In this graph the fraction of carbons following the pyruvate carboxylase pathway, f^{PC} , is assumed to be $f^{PC} = 0.2$. The ^{13}C labeling is normalized to the total amount of ^{13}C label going into the Krebs cycle.

Providing $[2,5-^{13}\text{C}_2]\text{glucose}$ or $[2-^{13}\text{C}]\text{pyruvate}$ to tissue/cells

Another way to determine how differently labeled glucose or pyruvate contribute to the production of citrate, $[2,5-^{13}\text{C}_2]\text{glucose}$ or $[2-^{13}\text{C}]\text{pyruvate}$ could be provided to epithelial tissue or prostate epithelial cells for a long enough period of time. Pyruvate is taken up by the cells and in this case the ^{13}C label will be located at a different pyruvate carbon position compared to the experiments with $[1,6-^{13}\text{C}_2]\text{glucose}$ or $[3-^{13}\text{C}]\text{pyruvate}$ (vide supra). When this ^{13}C label enters the Krebs cycle, it can end up at the oxaloacetate C2 and C3 position, via the pyruvate carboxylase route, or at the acetyl-CoA C1 position via the pyruvate dehydrogenase complex route. The first will result in a first labeling at C3 and C4 of citrate, the latter at C1. So, the ^{13}C carbon distribution in citrate at cycle turn $n = 0$ will look like (again, neglecting carbon dioxide for now):

$$\vec{C}(n=0) = \begin{pmatrix} c f^{PDC} \\ 0 \\ \frac{1}{2} f^{PC} \\ \frac{1}{2} f^{PC} \\ 0 \\ 0 \end{pmatrix} c \quad (9)$$

After one turn this distribution will have shifted again as described in section "Providing $[1,6-^{13}\text{C}_2]\text{glucose}$ or $[3-^{13}\text{C}]\text{pyruvate}$ to tissue/cells" (see also Table 1) and new label is added, via

the PDC route, at the C1 (via PDC) position of citrate every cycle turn.

$$\vec{C}(n=1) = \begin{pmatrix} cf^{PDC} \\ 0 \\ \frac{1}{4}f^{PC} \\ \frac{1}{4}f^{PC} \\ \frac{c}{2}f^{PDC} + \frac{1}{4}f^{PC} \\ \frac{c}{2}f^{PDC} + \frac{1}{4}f^{PC} \end{pmatrix} c(1-c) \quad (10)$$

From cycle turn $n \geq 2$ on the distribution at cycle turn n can be written in a more general way as

$$\vec{C}(n \geq 2) = \begin{pmatrix} cf^{PDC} \\ 0 \\ \frac{1}{2^{n+1}}f^{PC} \\ \frac{1}{2^{n+1}}f^{PC} \\ \frac{1}{2^{n+1}}f^{PC} + \frac{c}{2}f^{PDC} \\ \frac{1}{2^{n+1}}f^{PC} + \frac{c}{2}f^{PDC} \end{pmatrix} c(1-c)^n \quad (11)$$

The distribution of ^{13}C carbons over the carbons in the secreted citrate can be calculated again by calculating the sum of the contributions of all individual Krebs cycle turns n

$$\begin{aligned} \vec{C}_{distr}^{13\text{C}glc-2,5} &= \sum_{n=0}^{n=\infty} \vec{C}(n) = \begin{pmatrix} c \sum_{n=0}^{n=\infty} (1-c)^n f^{PDC} \\ 0 \\ \frac{1}{2} \sum_{i=0}^{i=\infty} \left(\frac{1-c}{2}\right)^i f^{PC} \\ \frac{1}{2} \sum_{i=0}^{i=\infty} \left(\frac{1-c}{2}\right)^i f^{PC} \\ \frac{c}{2} \sum_{i=1}^{i=\infty} (1-c)^i f^{PDC} + \frac{1}{2} \sum_{i=1}^{i=\infty} \left(\frac{1-c}{2}\right)^i f^{PC} \\ \frac{c}{2} \sum_{i=1}^{i=\infty} (1-c)^i f^{PDC} + \frac{1}{2} \sum_{i=1}^{i=\infty} \left(\frac{1-c}{2}\right)^i f^{PC} \end{pmatrix} c \\ &= \begin{pmatrix} f^{PDC} \\ 0 \\ \frac{1}{1+c}f^{PC} \\ \frac{1}{1+c}f^{PC} \\ \frac{1-c}{2} \left(\frac{1}{1+c}f^{PC} + f^{PDC} \right) \\ \frac{1-c}{2} \left(\frac{1}{1+c}f^{PC} + f^{PDC} \right) \end{pmatrix} c \end{aligned} \quad (12)$$

These equations give the steady state ^{13}C label distribution in citrate in the extracellular space or incubation medium after supplementation with $[2,5-^{13}\text{C}_2]\text{glucose}$ or $[2-^{13}\text{C}]\text{pyruvate}$. The distribution depends on the secretion fraction c and on the fractions of ^{13}C carbon entering the Krebs cycle via the pyruvate carboxylase route, f^{PC} , and via the pyruvate dehydrogenase complex route, f^{PDC} , (with $f^{PDC} = 1 - f^{PC}$). The distribution of ^{13}C carbons for $f^{PC} = 0.2$ is shown in Figure 8 plotted against secretion fraction c .

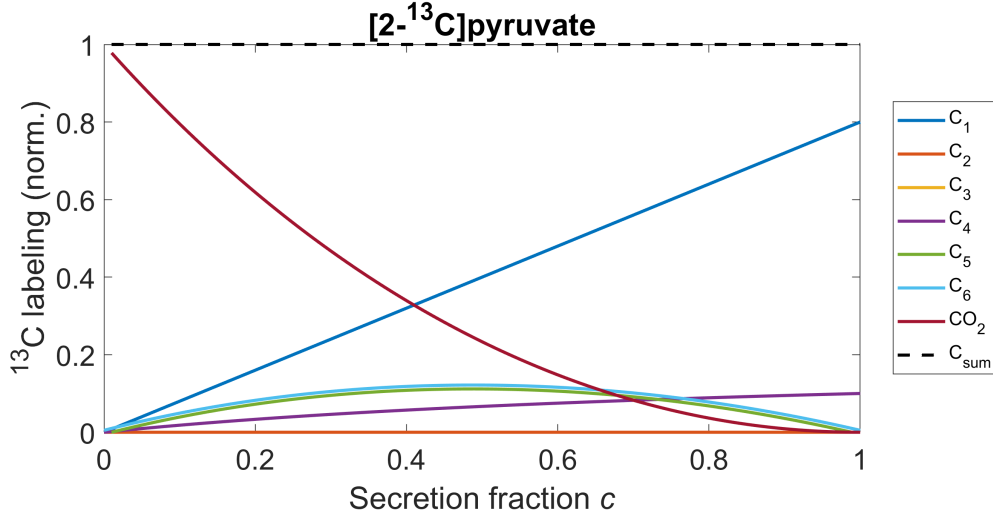


Figure 8: ^{13}C distribution over the six citrate carbons versus secretion fraction c after providing $[2,5-^{13}\text{C}_2]\text{glucose}$ or $[2-^{13}\text{C}]\text{pyruvate}$ to prostate epithelial tissue or cells. In this graph the fraction of carbons following the pyruvate carboxylase pathway, f^{PC} , is assumed to be $f^{PC} = 0.2$. The ^{13}C labeling is normalized to the total amount of ^{13}C label going into the Krebs cycle. Enrichments ϵ_p , ϵ_a and dilution fraction ϵ_c are assumed to be 1 here and no efflux of metabolites is taken into account apart from citrate secretion ($c = d$)

CO₂ production

Next to citrate production and secretion we also have to take into account how much carbon dioxide is produced every cycle and sum these contributions to see how much ^{13}C labels are lost as carbon dioxide. During a Krebs cycle turn one six-carbon molecule of citrate is converted into a four-carbon metabolite oxaloacetate and two carbons are lost as carbon dioxide. The first carbon is lost during the conversion of isocitrate into α -ketoglutarate and the second carbon is lost in the next step of the Krebs cycle during the conversion of α -ketoglutarate into succinyl-CoA. The first originates from the C6 carbon in citrate and the latter originates from citrate C5. So, the carbon dioxide production at cycle turn n is equal to the sum of citrate carbons C5 and C6 at this cycle turn n times $(1 - c)$ instead of times c since the production of carbon dioxide during cycle n takes place after the secretion of $(1 - c)^n$ citrate. In other words, only the ^{13}C carbons at C5 and C6, which are not secreted (fraction $(1 - c)^n$) at cycle n , are lost as carbon dioxide. This means we could calculate the carbon dioxide production at cycle turn n by summing the ^{13}C distribution at C5 and C6 and multiply this by $\frac{1-c}{c}$. Because the ^{13}C distribution at C5 and C6 is equal, this could be written as:

$$\overrightarrow{CO_2}(n) = 2 \frac{1-c}{c} \overrightarrow{C5}(n) \quad (13)$$

To calculate the resulting CO₂ produced over time the contributions of all cycle turns have to be summed.

$$\overrightarrow{CO_{2distr}} = \sum_{n=0}^{n=\infty} \overrightarrow{CO_2}(n) = 2 \frac{1-c}{c} \sum_{n=0}^{n=\infty} \overrightarrow{C5}(n) \quad (14)$$

Another way of calculating this is by evaluating the individual contributions for every cycle turn $\overrightarrow{CO_2}(n)$ to the total CO_2 for different values of n , like we did before for the carbons in citrate. For $[1,6-^{13}C_2]$ glucose or $[3-^{13}C]$ pyruvate this looks like:

$$\overrightarrow{CO_2}(n=0) = 0 \quad (15)$$

$$\overrightarrow{CO_2}(n=1) = 0 \quad (16)$$

$$\overrightarrow{CO_2}(n=2) = \frac{1}{2}f^{PC}(1-c)^2 \quad (17)$$

$$\overrightarrow{CO_2}(n \geq 3) = cf^{PDC} \sum_{i=1}^{i=n-2} \frac{(1-c)^n}{2^i} + \frac{(1-c)^n}{2^{n-1}}f^{PC} \quad (18)$$

This means we can calculate the total amount of CO_2 by summing these contributions:

$$\overrightarrow{CO_{2,distr}} = f^{PC} \sum_{n=2}^{n=\infty} \frac{(1-c)^n}{2^{n-1}} + cf^{PDC} \sum_{n=3}^{n=\infty} \sum_{i=1}^{i=n-2} \frac{(1-c)^n}{2^i} \quad (19)$$

$$= (1-c)^3 f^{PDC} - \frac{c(1-c)^3}{1+c} f^{PDC} + \frac{(1-c)^2}{1+c} f^{PC} \quad (20)$$

$$= \frac{2(1-c)}{c} \left[\frac{1-c}{2(1+c)} ((1-c)f^{PDC} + f^{PC}) c \right] \quad (21)$$

In the last step the equation has been rewritten to show that the total CO_2 indeed is equal to the final ^{13}C distribution at citrate C5 (or C6) times $2\frac{1-c}{c}$. Since the total ^{13}C entering the Krebs cycle in our model is equal to $f^{PC} + f^{PDC} = 1$ and we only take citrate production/secretion and CO_2 into account in our model the total ^{13}C found in citrate and CO_2 should also add up to 1. If we take the sum of the label distribution of the carbons of citrate and add the amount of CO_2 we should end up with $f^{PC} + f^{PDC} = 1$. For $[1,6-^{13}C_2]$ glucose or $[3-^{13}C]$ pyruvate this looks like:

$$\overrightarrow{Citr_{extr.cell.}^{glc-1,6,sum}} = cf^{PDC} \left(1 + 2\frac{1-c}{1+c} + \frac{(1-c)^2}{1+c} \right) + f^{PDC} \frac{(1-c)^3}{1+c} \quad (22)$$

$$+ cf^{PC} \left(\frac{2}{1+c} + \frac{1-c}{1+c} \right) + f^{PC} \frac{(1-c)^2}{1+c} \quad (23)$$

$$= f^{PDC} + f^{PC} = 1 \quad (24)$$

We can repeat this exercise for the addition of $[2,5-^{13}C_2]$ glucose or $[2-^{13}C]$ pyruvate. For this, we first have to take into account the values of $\overrightarrow{CO_2}(n)$ for different values of n , like we did before for the carbons in citrate:

$$\overrightarrow{CO_2}(n=0) = 0 \quad (25)$$

$$\overrightarrow{CO_2}(n=1) = 0 \quad (26)$$

$$\overrightarrow{CO_2}(n \geq 2) = (cf^{PDC} + \frac{1}{2^{n-1}}f^{PC})(1-c)^n \quad (27)$$

Now we can again calculate the total amount of CO₂ produced during the experiment by summing over n :

$$\overrightarrow{CO_2}_{distr} = cf^{PDC} \sum_{n=2}^{n=\infty} (1-c)^n + f^{PC} \sum_{n=2}^{n=\infty} \frac{(1-c)^n}{2^{n-1}} \quad (28)$$

$$= (1-c)^2 f^{PDC} + \frac{(1-c)^2}{1+c} f^{PC} \quad (29)$$

$$= 2 \frac{(1-c)}{c} \left(\frac{1-c}{2} \left(\frac{1}{1+c} f^{PC} + f^{PDC} \right) c \right) \quad (30)$$

So again the CO₂ production is equal to the sum of carbon labeling at citrate C5 and C6 times the factor $\frac{1-c}{c}$. The total amount of carbon entering the system has to be equal to the amount of carbon ending up in either citrate carbons or CO₂. If we take the sum of the labeling in the carbons of citrate and add the amount of CO₂ we should again end up with $f^{PC} + f^{PDC} = 1$. For [2,5-¹³C₂]glucose or [2-¹³C]pyruvate this looks like:

$$\overrightarrow{Citr}_{extr.cell.}^{glc-2,5,sum} = \left(\frac{2}{1+c} + \frac{1-c}{1+c} \right) cf^{PC} + \frac{(1-c)^2}{1+c} f^{PC} \quad (31)$$

$$+ (2-c)cf^{PDC} + (1-c)^2 f^{PDC} \quad (32)$$

$$= f^{PC} + f^{PDC} = 1 \quad (33)$$

So the total of ¹³C label entering the Krebs cycle is equal to the total ¹³C label we find after the experiment in citrate (extracellular or in the incubation medium) and in CO₂.

PDC versus PC contribution to citrate ¹³C-labeling

The equations we derived for the ¹³C distribution over citrate carbons after ¹³C substrate application can easily be split in separate contributions of the pyruvate carboxylase route and the pyruvate dehydrogenase complex route. For the application of [1,6-¹³C₂]glucose or [3-¹³C]pyruvate we arrive at the following expressions:

$$\overrightarrow{C}_{distr}^{13glc-1,6} = \begin{pmatrix} 0 \\ f^{PDC} \\ \frac{1-c}{1+c} f^{PDC} + \frac{1}{1+c} f^{PC} \\ \frac{1-c}{1+c} f^{PDC} + \frac{1}{1+c} f^{PC} \\ \frac{1-c}{2(1+c)} ((1-c)f^{PDC} + f^{PC}) \\ \frac{1-c}{2(1+c)} ((1-c)f^{PDC} + f^{PC}) \\ \frac{(1-c)^3}{c(1+c)} f^{PDC} + \frac{(1-c)^2}{c(1+c)} f^{PC} \end{pmatrix} c = \begin{pmatrix} 0 \\ 1 \\ \frac{1-c}{1+c} \\ \frac{1-c}{1+c} \\ \frac{(1-c)^2}{2(1+c)} \\ \frac{(1-c)^2}{2(1+c)} \\ \frac{(1-c)^3}{c(1+c)} \end{pmatrix} cf^{PDC} + \begin{pmatrix} 0 \\ 0 \\ \frac{1}{1+c} \\ \frac{1}{1+c} \\ \frac{1-c}{2(1+c)} \\ \frac{1-c}{2(1+c)} \\ \frac{(1-c)^2}{c(1+c)} \end{pmatrix} cf^{PC} \quad (34)$$

Note here that carbon dioxide is now also included in the vector (last value). And for the application of [2,5-¹³C₂]glucose or [2-¹³C]pyruvate we can do the same and end up with the

following equations:

$$\vec{^{13}C}_{distr}^{glc-2,5} = \begin{pmatrix} f^{PDC} \\ 0 \\ \frac{1}{1+c}f^{PC} \\ \frac{1}{1+c}f^{PC} \\ \frac{1-c}{2} \left(\frac{1}{1+c}f^{PC} + f^{PDC} \right) \\ \frac{1-c}{2} \left(\frac{1}{1+c}f^{PC} + f^{PDC} \right) \\ \frac{(1-c)^2}{c}f^{PDC} + \frac{(1-c)^2}{c(1+c)}f^{PC} \end{pmatrix} c = \begin{pmatrix} 1 \\ 0 \\ 0 \\ 0 \\ \frac{1-c}{2} \\ \frac{1-c}{2} \\ \frac{(1-c)^2}{c} \end{pmatrix} cf^{PDC} + \begin{pmatrix} 0 \\ 0 \\ \frac{1}{1+c} \\ \frac{1}{1+c} \\ \frac{1-c}{2(1+c)} \\ \frac{1-c}{2(1+c)} \\ \frac{(1-c)^2}{c(1+c)} \end{pmatrix} cf^{PC} \quad (35)$$

Overestimation of secretion fraction c

Next to citrate, other molecules are extracted from the Krebs cycle for other metabolic processes. This means that the fraction of citrate molecules remaining in the cycle will be smaller than $(1-c)$. Let's define an apparent citrate secretion fraction d which includes both citrate and other molecules (citrate equivalents) leaving the Krebs via other metabolic processes, for example in reactions involving aspartate and glutamate. So $d \geq c$ or $1-d \leq 1-c$. Now we can recalculate the equations derived earlier, first for $[1,6-^{13}C_2]$ glucose:

$$\vec{^{13}C}_{distr,app.secr.}^{glc-1,6} = \sum_{n=0}^{n=\infty} \left(\frac{1-d}{1-c} \right)^n \vec{C}(n) = \begin{pmatrix} 0 \\ df^{PDC} \sum_{j=0}^{j=\infty} (1-d)^j \\ df^{PDC} \sum_{j=1}^{j=\infty} \sum_{i=1}^{i=j} \frac{(1-d)^j}{2^i} + f^{PC} \sum_{j=0}^{j=\infty} \frac{(1-d)^j}{2^{j+1}} \\ df^{PDC} \sum_{j=1}^{j=\infty} \sum_{i=1}^{i=j} \frac{(1-d)^j}{2^i} + f^{PC} \sum_{j=0}^{j=\infty} \frac{(1-d)^j}{2^{j+1}} \\ df^{PDC} \sum_{j=2}^{j=\infty} \sum_{i=2}^{i=j} \frac{(1-d)^j}{2^i} + f^{PC} \sum_{j=0}^{j=\infty} \frac{(1-d)^j}{2^{j+1}} \\ df^{PDC} \sum_{j=2}^{j=\infty} \sum_{i=2}^{i=j} \frac{(1-d)^j}{2^i} + f^{PC} \sum_{j=0}^{j=\infty} \frac{(1-d)^j}{2^{j+1}} \end{pmatrix} c \quad (36)$$

$$= \begin{pmatrix} 0 \\ f^{PDC} \\ \frac{1-d}{1+d}f^{PDC} + \frac{1}{1+d}f^{PC} \\ \frac{1-d}{1+d}f^{PDC} + \frac{1}{1+d}f^{PC} \\ \frac{1-d}{2(1+d)} \left((1-d)f^{PDC} + f^{PC} \right) \\ \frac{1-d}{2(1+d)} \left((1-d)f^{PDC} + f^{PC} \right) \end{pmatrix} c$$

For [2,5-¹³C₂]glucose or [2-¹³C]pyruvate we can do the same:

$$\begin{aligned}
\overrightarrow{{}^{13}\text{C}_{distr,app.secr.}^{glc-2,5}} &= \sum_{n=0}^{n=\infty} \left(\frac{1-d}{1-c} \right)^n \overrightarrow{\text{C}}(n) = \begin{pmatrix} d \sum_{n=0}^{n=\infty} (1-d)^n f^{PDC} \\ 0 \\ \frac{1}{2} \sum_{i=0}^{i=\infty} \left(\frac{1-d}{2} \right)^i f^{PC} \\ \frac{1}{2} \sum_{i=0}^{i=\infty} \left(\frac{1-d}{2} \right)^i f^{PC} \\ \frac{d}{2} \sum_{i=1}^{i=\infty} (1-d)^i f^{PDC} + \frac{1}{2} \sum_{i=1}^{i=\infty} \left(\frac{1-d}{2} \right)^i f^{PC} \\ \frac{d}{2} \sum_{i=1}^{i=\infty} (1-d)^i f^{PDC} + \frac{1}{2} \sum_{i=1}^{i=\infty} \left(\frac{1-d}{2} \right)^i f^{PC} \end{pmatrix}^c \\
&= \begin{pmatrix} f^{PDC} \\ 0 \\ \frac{1}{1+d} f^{PC} \\ \frac{1}{1+d} f^{PC} \\ \frac{1-d}{2} \left(\frac{1}{1+d} f^{PC} + f^{PDC} \right) \\ \frac{1-d}{2} \left(\frac{1}{1+d} f^{PC} + f^{PDC} \right) \end{pmatrix}^c
\end{aligned} \tag{37}$$

The resulting equations are similar to the equations obtained earlier, but c is replaced by d everywhere and then all equations are multiplied by $\frac{c}{d}$. Taking this into account in the curves in figures 7 and 8, would mean that they have d instead of c on the x-axis, and are scaled with factor c/d .

¹³C-enrichment of pyruvate and acetyl-CoA pool

Until now, we assumed the ¹³C-enrichment of the pyruvate and acetyl-CoA to be 100%. This does not represent the real situation in cells or tissue, therefore we introduce enrichment fractions ϵ_p and ϵ_a . All equations are multiplied with ϵ_p and the terms involving carbons flowing via the PDC route are multiplied additionally with ϵ_a . Another potential factor to take into consideration is the fast exchange between citrate, isocitrate and α -ketoglutarate. During this exchange the C6 of citrate is exchanged with free CO₂, which potentially is unlabeled. If there's any ¹³C labeling at C6, this might be diluted by this exchange with unlabeled CO₂. To take the effect of this exchange on the citrate C6 level into account, a dilution factor ϵ_c is introduced. For [1,6-¹³C₂]glucose or [3-¹³C]pyruvate this comes down to:

$$\overrightarrow{{}^{13}\text{C}_{distr}^{glc-1,6}} = \begin{pmatrix} 0 \\ \epsilon_a f^{PDC} \\ \frac{(1-d)\epsilon_a}{1+d} f^{PDC} + \frac{1}{1+d} f^{PC} \\ \frac{(1-d)\epsilon_a}{1+d} \epsilon_a f^{PDC} + \frac{1}{1+d} f^{PC} \\ \frac{1-d}{2(1+d)} \left((1-d)\epsilon_a f^{PDC} + f^{PC} \right) \\ \frac{(1-d)\epsilon_c}{2(1+d)} \left((1-d)\epsilon_a f^{PDC} + f^{PC} \right) \\ \frac{(1-d)^3 \epsilon_a}{d(1+d)} f^{PDC} + \frac{(1-d)^2}{d(1+d)} f^{PC} \end{pmatrix} \epsilon_p d \tag{38}$$

And for $[2,5-^{13}\text{C}_2]\text{glucose}$ or $[2-^{13}\text{C}]\text{pyruvate}$ this would be:

$$\vec{^{13}\text{C}}_{\text{glc-2,5}}^{\text{distr}} = \begin{pmatrix} \epsilon_a f^{PDC} \\ 0 \\ \frac{1}{1+d} f^{PC} \\ \frac{1}{1+d} f^{PC} \\ \frac{1-d}{2} \left(\frac{1}{1+d} f^{PC} + \epsilon_a f^{PDC} \right) \\ \frac{(1-d)\epsilon_c}{2} \left(\frac{1}{1+d} f^{PC} + \epsilon_a f^{PDC} \right) \\ \frac{(1-d)^2 \epsilon_a}{d} f^{PDC} + \frac{(1-d)^2}{d(1+d)} f^{PC} \end{pmatrix} \epsilon_p d \quad (39)$$

Mass balance

The efflux of other metabolites confined in the apparent secretion fraction d does not mean that there is actually a fraction d of Krebs cycle metabolites lost every cycle, but rather shows how much ^{13}C labeled citrate equivalents are either diverged from the cycle or exchanged for unlabeled metabolites. This means that even if there's low influx of carbons via pyruvate carboxylase (f^{PC}), there's still citrate secretion possible, as long as the Krebs cycle is supplied sufficiently with carbons from unlabeled molecules (like glutamine, glutamate and aspartate). The apparent secretion fraction d therefore tells us something about both citrate diverging from the Krebs cycle, citrate equivalent diverging from the Krebs cycle and the exchange of labeled molecules with unlabeled molecules (e.g. in the α -ketoglutarate and (rather large) glutamate pool).

Calculation of secretion fraction c and PC fraction f^{PC}

Experimental ratios

From the equations obtained in sections "Providing $[2,5-^{13}\text{C}_2]\text{glucose}$ or $[2-^{13}\text{C}]\text{pyruvate}$ to tissue/cells" and "Providing $[1,6-^{13}\text{C}_2]\text{glucose}$ or $[3-^{13}\text{C}]\text{pyruvate}$ to tissue/cells" (also summarized in Table 2) we can define experimental ratios of ^{13}C citrate signal integrals which can be easily obtained from ^{13}C MR spectra. Since citrate C2 and C4 on one hand and C1 and C5 on the other are chemically equivalent, we only have to consider ratios composed of C1/5, C2/4, C3 and C6. We suggest the following experimental ratios of fitted ^{13}C citrate integrals to be used because they consist of the carbons with the highest signal intensity (and consequently SNR), for most of the values of c : R_1 for $[1,6-^{13}\text{C}_2]\text{glucose}$ or $[3-^{13}\text{C}]\text{pyruvate}$ experiments.

$$R_1 = \frac{(C_2 + C_4) - C_3}{(C_2 + C_4)} \quad (40)$$

The reason for choosing this ratio is that, when looking at the equations derived for the ^{13}C distribution over the citrate, C3 and C4 have equal signal intensities. By subtracting C3 from C2+C4 (one peak) we get C2, so R_1 reports on the fraction that C2 makes up of C2+C4. For the $[2,5-^{13}\text{C}_2]\text{glucose}$ or $[2-^{13}\text{C}]\text{pyruvate}$ experiments we suggest R_2 .

$$R_2 = \frac{C_1 + C_5}{C_3} \quad (41)$$

These ratios can then be used as experimental input values for the quantitative model we derived in this work describing citrate production and secretion in prostate epithelial tissue or cell

lines. After providing prostate tissue or cells either with [1,6-¹³C₂]glucose or [3-¹³C]pyruvate or with [2,5-¹³C₂]glucose or [2-¹³C]pyruvate, the extracellular material, being extracellular fluid or incubation medium, can be analyzed using ¹³C NMR spectroscopy. After identification and quantification of the citrate resonance peaks the two ratios, defined above, can be calculated. These are then used to calculate secretion fraction c and pyruvate carboxylase contribution f^{PC} as described below.

Real citrate secretion fraction c

With ratio R_1 (from the [1,6-¹³C₂]glucose or [3-¹³C]pyruvate experiments) and ratio R_2 (from the [2,5-¹³C₂]glucose or [2-¹³C]pyruvate experiments) we can calculate the secretion fraction. First we rewrite the equation for R_1 :

$$R_1 = \frac{C_{2/4} - C_3}{C_{2/4}} = \frac{C_2 + C_4 - C_3}{C_2 + C_4} = \frac{f^{PDC} + \frac{1-c}{1+c}f^{PDC} + \frac{1}{1+c}f^{PC} - \frac{1-c}{1+c}f^{PDC} - \frac{1}{1+c}f^{PC}}{f^{PDC} + \frac{1-c}{1+c}f^{PDC} + \frac{1}{1+c}f^{PC}} \quad (42)$$

From [2,5-¹³C₂]glucose or [2-¹³C]pyruvate experiments we can calculate ratio R_2 :

$$R_2 = \frac{C_{1/5}}{C_3} = \frac{C_1 + C_5}{C_3} = \frac{f^{PDC} + \frac{1-c}{2} \left(\frac{1}{1+c}f^{PC} + f^{PDC} \right)}{\frac{1}{1+c}f^{PC}} \quad (43)$$

This can be simplified by extracting an equation for f^{PDC} dependent on c and R_1 ,

$$f^{PDC} = \frac{R_1}{(1+c) - R_1} \quad (44)$$

and substituting this into the equation for R_2 :

$$R_2 = \frac{\frac{R_1}{1+c-R_1} + \frac{1-c}{2} \left(\frac{1}{1+c} \left(1 - \frac{R_1}{1+c-R_1} \right) + \frac{R_1}{1+c-R_1} \right)}{\frac{1}{1+c} \left(1 - \frac{R_1}{1+c-R_1} \right)} \quad (45)$$

This can now be solved for c by rewriting this into a quadratic equation:

$$-(R_1 + 1)c^2 + (4R_1 - 2R_2)c + (R_1 - 2R_2 + 4R_1R_2 + 1) = 0 \quad (46)$$

After substituting values for R_1 and R_2 in this quadratic equation, we can solve for c . For example, for for $c = 0.3$ and $f^{PC} = 0.2$, R_1 would be ≈ 0.58 and R_2 would be ≈ 7.37 , filling this in gives:

$$-1.58c^2 - 12.43c + 3.87 = 0 \quad (47)$$

Solving the quadratic equation of course gives us back $c = 0.3$.

Fraction f^{PC} versus f^{PDC}

Now, using the expression we derived above we can calculate the fractions f^{PDC} and f^{PC} :

$$f^{PDC} = \frac{R_1}{1+c-R_1} \quad (48)$$

$$f^{PC} = 1 - f^{PDC} \quad (49)$$

Using the values for c and f^{PC} we can calculate the total integrals of the citrate and carbon dioxide carbons according to equations 34 and 35 (see also Figures 9 and 10). Looking at the predicted ^{13}C integrals for the different citrate carbons assuming $c = 0.3$ and $f^{PC} = 0.2$, we can see that indeed C2/4 and C3 in the $[1,6-^{13}\text{C}_2]$ glucose or $[3-^{13}\text{C}]$ pyruvate experiment is the best choice taking into account SNR, and for the $[2,5-^{13}\text{C}_2]$ glucose or $[2-^{13}\text{C}]$ pyruvate experiment the $\text{C}_{1/5}$ and C_3 or C_6 signals would be best to evaluate. However, often the peak of citrate C_6 overlaps with another peak in the ^{13}C spectrum (e.g. pyroglutamate), making C_3 the best choice.

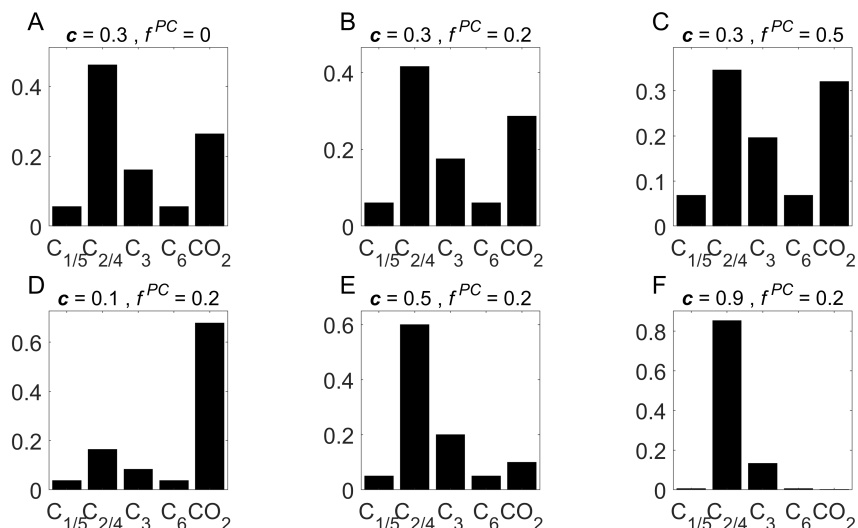


Figure 9: Relative ^{13}C NMR signal integrals of the six citrate carbons and carbon dioxide for different values of f^{PC} with $c = 0.3$ (A-C), and different values of c with $f^{PC} = 0.2$ (D-F), after the application of $[1,6-^{13}\text{C}_2]$ glucose or $[3-^{13}\text{C}]$ pyruvate to prostate epithelial tissue or cells. Carbons C1 and C5, and C2 and C4 have the same chemical shift and their signal integrals are therefore summed here. In these figures, the pyruvate and acetyl-CoA pool are assumed to be fully labeled and no other efflux of metabolites/citrate equivalents are taken into account.

Average number of Krebs cycle turns

Using equation 4 derived in section "Average number of completed Krebs cycle turns before citrate secretion" the average number of Krebs cycle turns that are completed before secretion of a citrate molecule can be calculated:

$$\langle n \rangle = \sum_{n=0}^{n=\infty} nc(1-c)^n = \frac{1-c}{c} \quad (50)$$

Pyruvate carboxylase fraction dependence on secretion fraction

In section "Fraction f^{PC} versus f^{PDC} " (vide supra) an expression was derived for fractions f^{PDC} and f^{PC} (using $f^{PC} = 1 - f^{PDC}$) depending on c and R_1 (Equation 49). We can derive

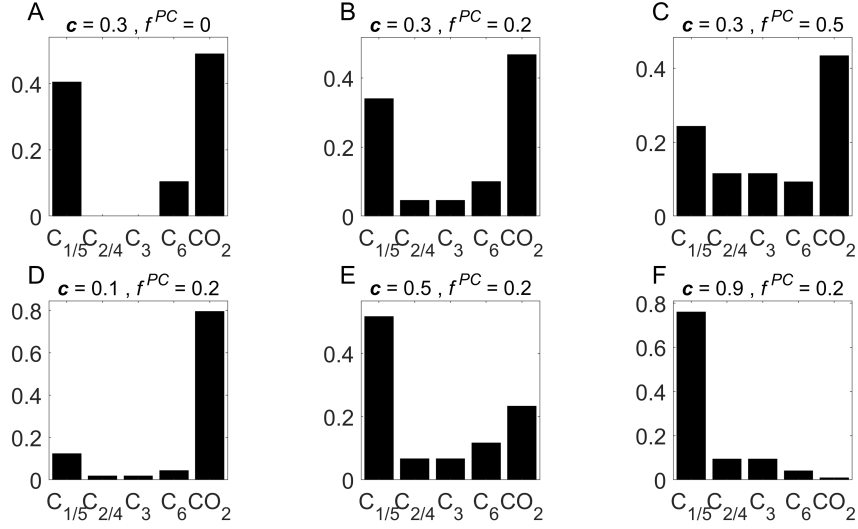


Figure 10: Relative ^{13}C NMR signal integrals of the six citrate carbons and carbon dioxide for different values of f^{PC} with $c = 0.3$ (A-C), and different values of c with $f^{PC} = 0.2$ (D-F), after application of $[2,5-^{13}\text{C}_2]$ glucose or $[2-^{13}\text{C}]$ pyruvate to prostate epithelial tissue or cells. Carbons C1 and C5, and C2 and C4 have the same chemical shift and their signal integrals are therefore summed here. In these figures, the pyruvate and acetyl-CoA pool are assumed to be fully labeled and no other efflux of metabolites/citrate equivalents are taken into account.

a similar equation for f^{PC} only depending on c and R_2 .

$$R_2 = \frac{C_{1/5}}{C_3} = \frac{C_1 + C_5}{C_3} = \frac{f^{PDC} + \frac{1-c}{2} \left(\frac{1}{1+c} f^{PC} + f^{PDC} \right)}{\frac{1}{1+c} f^{PC}} \quad (51)$$

$$f^{PC} = \frac{(1+c)(3-c)}{2(R_2+1) + (3-c)c} \quad (52)$$

Using this and equation 49, we can plot c versus f^{PC} for different values of R_1 and R_2 (Figure 11). The intersection of the lines for R_1 and R_2 represent a unique combination of secretion fraction c and pyruvate carboxylase fraction f^{PC} , derived from these ratios of ^{13}C NMR signal intensities of citrate carbons.

Error propagation

The experimental ratios obtained in ^{13}C experiments are subject to errors due to SNR limitations of the spectra and this has its effect on variability of the values for c and f^{PC} that we calculated. Assuming a standard deviation equal to 1%, 2% or 4% of the largest signal integral (e.g. C2) for all components in the ratio (in a way similar to relative noise levels of 1%, 2% and 4%) we calculated the error propagation for c and f^{PC} . For $c = 0.3$ and $f^{PC} = 0.2$ the error bounds are presented in figure 12. A large spread in possible values for c is seen at increasing error, while a more moderate spread is observed in values for f^{PC} .

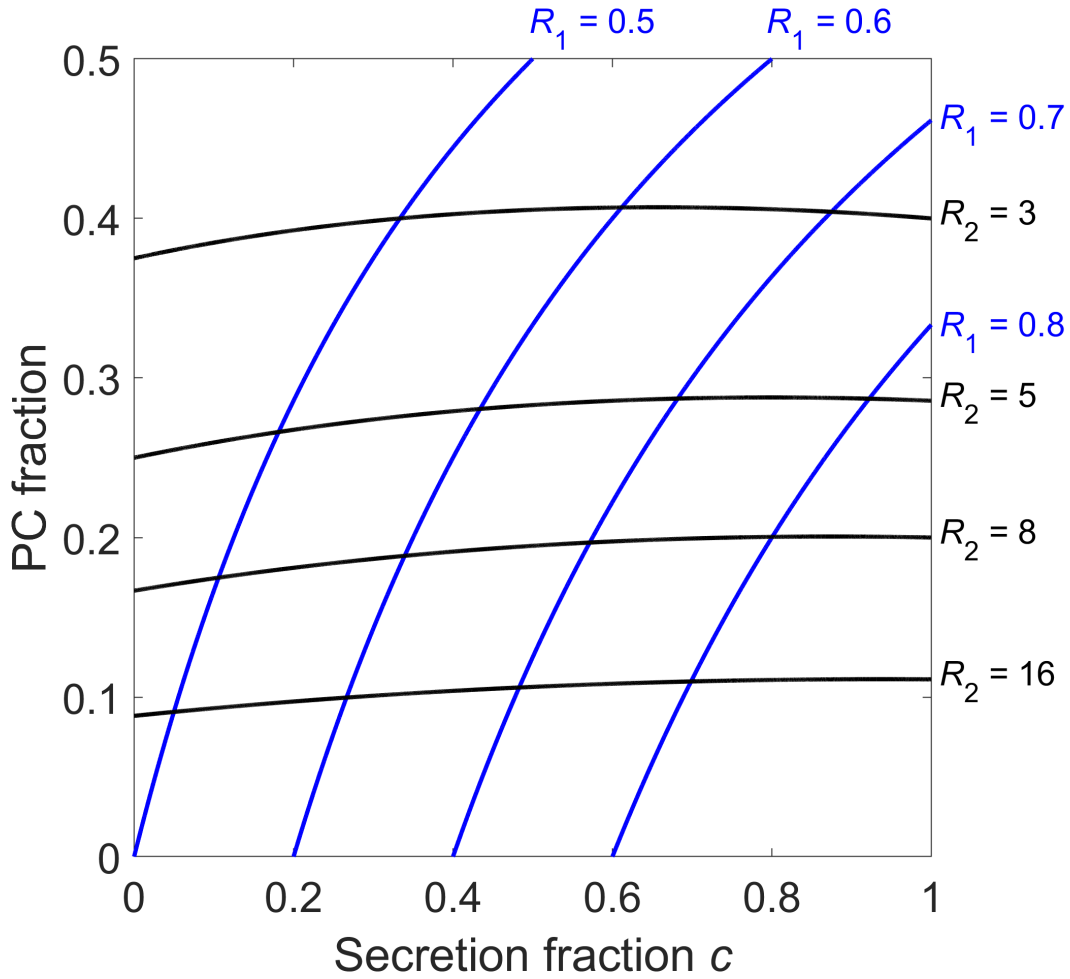


Figure 11: Fraction pyruvate carboxylase f^{PC} versus secretion fraction c with lines representing different values for R_1 and R_2 .

Efflux from the Krebs cycle of other metabolites in addition to citrate and different pool ^{13}C -enrichments

Secretion fraction with efflux of other metabolites in addition to citrate

In the previous sections we neglected the contributions of other metabolic pathways (both cataplerotic and anaplerotic), connected to the Krebs cycle carbon pool, in the efflux of carbons from this cycle. To take this into account we introduced an 'apparent citrate secretion fraction d ' in the section "Overestimation of secretion fraction c " covering all contributions to the efflux of metabolites from the Krebs cycle. We also assumed equal (full) ^{13}C -enrichment of the pyruvate and acetyl-CoA pools. We can use the results in Equations 38 and 39 to recalculate the results and see what the effect of these parameters is. Using R_1 and R_2 and the equations in this section (Eq. 36 and 37) we can only calculate the total fraction of molecules flowing out of the Krebs

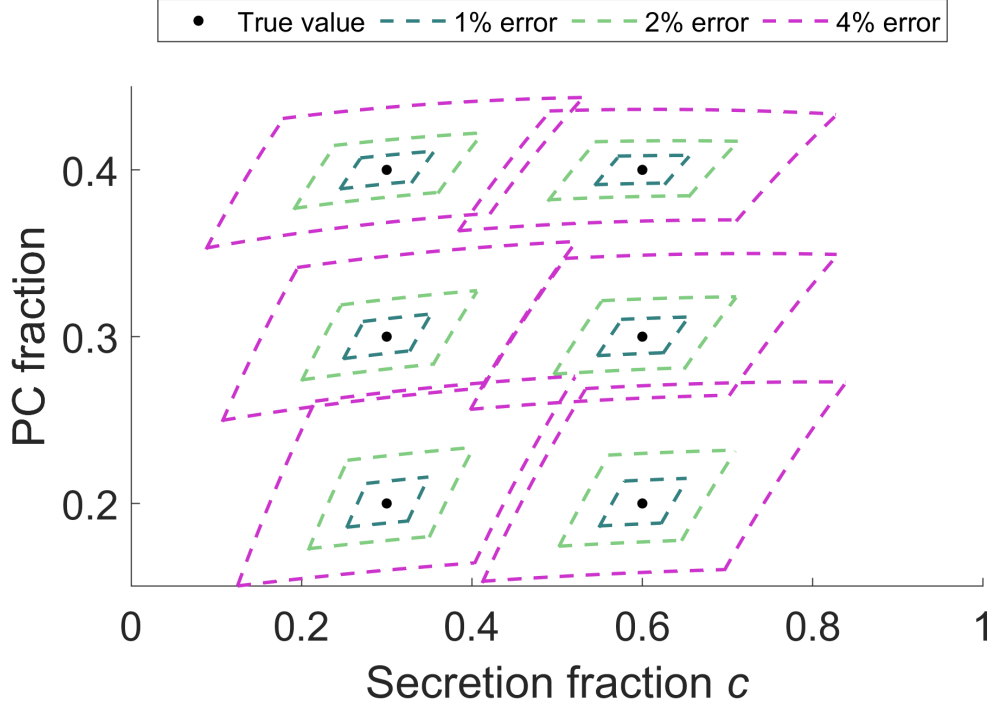


Figure 12: Confidence intervals for pyruvate carboxylase fraction f^{PC} and secretion fraction c at different error levels. These intervals are shown for $f^{PC} = 0.2$, $f^{PC} = 0.3$ and $f^{PC} = 0.4$, and for the secretion fraction $c = 0.3$ and $c = 0.6$. Confidence intervals were calculated for errors (or noise levels) of 1%, 2% and 4% of the biggest integral in the equations for R_1 and R_2 (From the equations derived in sections "Providing $[1,6-^{13}C_2]$ glucose or $[3-^{13}C]$ pyruvate to tissue/cells" and "Providing $[2,5-^{13}C_2]$ glucose or $[2-^{13}C]$ pyruvate to tissue/cells" follows that $C_{2/4}$ is the largest integral for R_1 and $C_{1/5}$ for R_2 for all physical values of c and f^{PC}).

cycle, d . Within the current experimental scope we cannot separate secretion of citrate from other pathways transporting carbons out of the Krebs cycle. Still, we can assume $c \leq d$. An expression for R_1 including d and the enrichment fractions is as follows:

$$R_1 = \frac{C_{2/4} - C_3}{C_{2/4}} = \frac{C_2 + C_4 - C_3}{C_2 + C_4} = \frac{\epsilon_a f^{PDC} + \frac{1-d}{1+d} \epsilon_a f^{PDC} + \frac{1}{1+d} f^{PC} - \frac{1-d}{1+d} \epsilon_a f^{PDC} - \frac{1}{1+d} f^{PC}}{\epsilon_a f^{PDC} + \frac{1-d}{1+d} \epsilon_a f^{PDC} + \frac{1}{1+d} f^{PC}} \frac{\epsilon_p}{\epsilon_p} \quad (53)$$

We can now again rewrite the expression to obtain f^{PDC} as a function of d and R_1 :

$$f^{PDC} = \frac{R_1}{\epsilon_a(1+d) - R_1(2\epsilon_a - 1)} \quad (54)$$

From the $[2,5-^{13}C_2]$ glucose or $[2-^{13}C]$ pyruvate experiments we can calculate ratio R_2 :

$$R_2 = \frac{C_{1/5}}{C_3} = \frac{C_1 + C_5}{C_3} = \frac{\epsilon_a f^{PDC} + \frac{1-d}{2} \left(\frac{1}{1+d} f^{PC} + \epsilon_a f^{PDC} \right)}{\frac{1}{1+d} f^{PC}} \frac{\epsilon_p}{\epsilon_p} \quad (55)$$

Substituting values for R_1 and R_2 we can now solve for d

$$-\epsilon_a(R_1 + 1)d^2 + \epsilon_a(4R_1 - 2R_2)d + \epsilon_a(R_1 - 2R_2 + 4R_1R_2 + 1) = 0 \quad (56)$$

Taking into account additional efflux of carbons from the Krebs cycle (Difference between apparent citrate secretion fraction d and true citrate secretion fraction c), the real secretion fraction for citrate c is evidently smaller or equal to the value found for d .

Fraction f^{PC} versus f^{PDC} with efflux of other metabolites

Above we presented an expression of fraction f^{PDC} , taking into account other efflux of citrate equivalents in an apparent secretion fraction d . We can derive an expression for f^{PC} :

$$f^{PDC} = \frac{R_1}{\epsilon_a(1 + d) - R_1(2\epsilon_a - 1)} \quad (57)$$

$$f^{PC} = 1 - f^{PDC}$$

Taking into account other efflux besides citrate from the Krebs cycle, fortunately does not affect the values calculated for f^{PC} or f^{PDC} .

Average number of Krebs cycle turns including efflux of citrate equivalents/other molecules d

An expression for the average number of completed cycle turns before secretion of a citrate molecule, taking an apparent secretion fraction d into account, is straightforwardly obtained by replacing c for d .

$$\langle n \rangle = \sum_{n=0}^{n=\infty} nd(1-d)^n = \frac{1-d}{d} \quad (58)$$

True citrate secretion fraction c versus apparent citrate secretion fraction d

It is not possible to distinguish c and d from each other within the experimental scope for which our model is designed, but we do know that the secretion fraction c has to be smaller than d if there is carbon, in addition to citrate carbons, flowing out of the Krebs cycle. So less than the calculated fraction d of citrate molecules are secreted every cycle turn. The average number of completed cycle turns before secretion of citrate, in the situation that there are no other processes involved, would be even larger.

$$\begin{aligned}
\vec{C}_{distr}^{13} &= \vec{C}(0) + \vec{C}(1) + \vec{C}(2) + \vec{C}(3) + \dots = \sum_{n=0}^{n=\infty} \vec{C}(n) \\
\vec{C}_{distr}^{glc-1,6} &= \begin{pmatrix} 0 \\ c f^{PDC} \\ \frac{c}{2} f^{PC} + \frac{1}{2} f^{PC} \\ \frac{c}{2} f^{PDC} + \frac{1}{4} f^{PC} \\ 0 \\ 0 \\ 0 \end{pmatrix} + \begin{pmatrix} 0 \\ c f^{PDC} \\ \frac{3c}{4} f^{PDC} + \frac{1}{8} f^{PC} \\ \frac{3c}{4} f^{PDC} + \frac{1}{8} f^{PC} \\ \frac{c}{4} f^{PDC} + \frac{1}{8} f^{PC} \\ \frac{c}{4} f^{PDC} + \frac{1}{8} f^{PC} \\ \frac{1}{2c} f^{PC} \end{pmatrix} + \begin{pmatrix} 0 \\ c f^{PDC} \\ \frac{7c}{8} f^{PDC} + \frac{1}{16} f^{PC} \\ \frac{7c}{8} f^{PDC} + \frac{1}{16} f^{PC} \\ \frac{3c}{8} f^{PDC} + \frac{1}{16} f^{PC} \\ \frac{3c}{8} f^{PDC} + \frac{1}{16} f^{PC} \\ \frac{1}{2} f^{PDC} + \frac{1}{4c} f^{PC} \end{pmatrix} + \dots = \begin{pmatrix} 0 \\ f^{PDC} \\ \frac{1-c}{1+c} f^{PDC} + \frac{1}{1+c} f^{PC} \\ \frac{1-c}{1+c} f^{PDC} + \frac{1}{1+c} f^{PC} \\ \frac{1-c}{2(1+c)} ((1-c) f^{PDC} + f^{PC}) \\ \frac{1-c}{2(1+c)} ((1-c) f^{PDC} + f^{PC}) \\ \frac{(1-c)^3}{c(1+c)} f^{PDC} + \frac{(1-c)^2}{c(1+c)} f^{PC} \end{pmatrix} \\
\vec{C}_{distr}^{glc-2,5} &= \begin{pmatrix} c f^{PDC} \\ 0 \\ \frac{1}{2} f^{PC} \\ \frac{1}{2} f^{PC} \\ 0 \\ 0 \\ 0 \end{pmatrix} + \begin{pmatrix} c f^{PDC} \\ 0 \\ \frac{1}{8} f^{PC} \\ \frac{1}{8} f^{PC} \\ \frac{c}{2} f^{PDC} + \frac{1}{8} f^{PC} \\ \frac{c}{2} f^{PDC} + \frac{1}{8} f^{PC} \\ f^{PDC} + \frac{1}{2c} f^{PC} \end{pmatrix} + \begin{pmatrix} c f^{PDC} \\ 0 \\ \frac{1}{16} f^{PC} \\ \frac{1}{16} f^{PC} \\ \frac{c}{2} f^{PDC} + \frac{1}{16} f^{PC} \\ \frac{c}{2} f^{PDC} + \frac{1}{16} f^{PC} \\ f^{PDC} + \frac{1}{4c} f^{PC} \end{pmatrix} + \dots = \begin{pmatrix} c f^{PDC} \\ 0 \\ \frac{1}{1+c} f^{PC} \\ \frac{1}{1+c} f^{PC} \\ \frac{1-c}{2} \left(\frac{1}{1+c} f^{PC} + f^{PDC} \right) \\ \frac{1-c}{2} \left(\frac{1}{1+c} f^{PC} + f^{PDC} \right) \\ \frac{(1-c)^2}{c} f^{PDC} + \frac{(1-c)}{c(1+c)} f^{PC} \end{pmatrix}
\end{aligned}$$

Table 2: The ^{13}C distributions over six citrate carbons and carbon dioxide for the Krebs cycle turns $n = 0 - 3$ and their summation. Top row is after providing prostate epithelial cells or tissue with $[1,6-^{13}\text{C}_2]\text{glucose}$ or $[3-^{13}\text{C}]\text{pyruvate}$ and bottom row shows the result after providing $[2,5-^{13}\text{C}_2]\text{glucose}$ or $[2-^{13}\text{C}]\text{pyruvate}$.

Discussion & Conclusions

In this paper we present a quantitative model describing metabolic pathways in the production of labeled citrate in the mitochondria of prostatic epithelial cells and its secretion into the luminal space or incubation medium. Our model focuses on the application of ^{13}C labeled substrates and the distribution of ^{13}C labels over the 6 carbons in secreted citrate as a read-out for intracellular metabolism. In the design of the model we have taken common characteristics of the Krebs cycle into account such as the rapid carbon exchange between oxaloacetate, malate and fumarate.^{41,42} We show how to calculate the fraction of citrate leaving the Krebs cycle for secretion, i.e. c , and how to calculate the fractions of pyruvate dehydrogenase complex (PDC) versus the anaplerotic pyruvate carboxylase (PC) pathway in supplying the Krebs cycle with carbons from pyruvate, i.e. f^{PC} and f^{PDC} . For this purpose we suggest two simple ratios of ^{13}C NMR signal integrals of citrate that can be obtained after supplementation with ^{13}C labeled glucose or pyruvate to prostate tissue *in vivo* or cell lines *in vitro*. These measures are shown to be independent of ^{13}C -enrichment of the administered supplements. Since the total NMR integrals of the citrate carbons are measured, the model is independent of ^{13}C J-coupling patterns, making this method more robust if SNR is low. It can be adjusted for use with other ^{13}C labeled supplements, especially if those are feeding the acetyl-CoA pool.

For this model we assumed that the ^{13}C pool of glucose and pyruvate are large compared to the Krebs cycle ^{13}C pool, which results in an average constant flow of ^{13}C labels entering the Krebs cycle over time. Another assumption made in deriving this model is the constant secretion fraction of citrate over time. If the tissue or cells are provided with a constant flow of ^{13}C label for a long period of time, we can assume that the epithelial cells on average are in a steady state with respect to citrate production and general metabolism during this period.

After citrate diverges from the Krebs cycle and is transported to the cytosol it can be used in *de novo* lipid synthesis and in further metabolic conversions. Assuming lipid synthesis and secretion of citrate by the transporters out of the cells is constant over time this doesn't influence the ^{13}C labeling pattern found for citrate in the extracellular fluid or incubation medium since an equal fraction of all citrate present in the cytosol will be lost to lipid synthesis or other metabolism independent of the ^{13}C labeling of citrate. Only if the ^{13}C labels subsequently end up in the Krebs cycle again this could influence the final outcome of the experiments, but we assume this to be negligible.

Initially we assumed that, apart from secretion of citrate and carbon dioxide, no other efflux of carbons occurs during each cycle turn. In this way we derived an expression for the average true citrate secretion fraction c . However, carbons may leave the Krebs cycle elsewhere. Thus, the secretion fraction calculated from experimental values using this model concerns the total fraction of molecules diverging from the Krebs cycle during one cycle turn, not only citrate. We show that the efflux of other metabolites does not have an effect on the value of f^{PC} or f^{PDC} but it does result in an overestimation of secretion fraction c . To take this into account we introduce an apparent secretion fraction d , which represents Krebs cycle efflux of carbons from citrate and other molecules and thus gives an upper value for the secretion of citrate. Efflux from the Krebs cycle pool can be due to for example conversion of α -ketoglutarate into glutamate by glutamate dehydrogenase, pyruvate production from oxaloacetate via PEPCK and aspartate transaminase activity. The latter is part of the malate-aspartate shuttle and catalyzes the conversion of α -ketoglutarate into glutamate and of oxaloacetate into aspartate, and contributes to the efflux of metabolites from the Krebs cycle for production of amino acids and proteins. Multiple metabolic flux modeling studies have calculated total Krebs cycle fluxes and net influx and efflux from the

Krebs cycle. In some cases exchange fluxes were calculated in addition to net fluxes. Especially interesting is the high exchange flux associated with the exchange between α -ketoglutarate and glutamate, which can be comparable to total Krebs cycle fluxes *in vivo* in tissues like heart^{25,27} and brain^{24,28–30}, but also *in vitro* in metastatic cell lines like melanoma^{17,18}, hepatocyte and hepatoma²³ and glioma¹⁹ cells. Depending on the size of the unlabeled glutamate pool this can result in a fast isotopical dilution of the α -ketoglutarate pool, resulting in loss of ¹³C labeled carbon skeletons. These processes and possibly further loss of ¹³C-labeled Krebs cycle metabolites accounts for the total efflux of ¹³C carbons from the Krebs cycle. Until now no literature values for similar exchange fluxes are available for prostate tissues or cell systems. Future efforts can be made to extend the model with an estimation of loss of ¹³C labeled carbon skeletons to glutamate using the intracellular glutamate pool size and (relative) exchange fluxes. The ¹³C-enrichment of the pyruvate and acetyl-CoA pool are taken into consideration as well, assuming these to be equal leads to an overestimation of the fraction f^{PC} . Therefore it is needed to include analysis of enrichments of these pools into experimental setups.

The high labeling efficiency of citrate using the ¹³C substrates described here make these substrates ideal candidates for studying metabolism underlying the unique secretion of citrate by prostate tissue. Still, extending this model to other ¹³C labeled substrates or other isotopes like ¹⁴C or ²H would open windows on more details of this metabolism.

In the context of our model we propose ratios of ¹³C NMR signals of citrate, R_1 and R_2 , as read-out indices of metabolism involved in citrate production and secretion in prostatic tissue. From these indices we can calculate Krebs cycle efflux or true citrate secretion fraction c (or apparent citrate secretion fraction d) and the fraction of pyruvate carbons entering the Krebs cycle via the PC or PDC routes. A change in these indices could indicate a shift in metabolism associated with the development of prostate diseases, such as prostate cancer, and could be used to probe therapy effectiveness. For this it would be necessary to first measure baseline indices in healthy prostate tissue by measuring citrate secreted by healthy epithelial tissue *in vivo* and secondly determine how much these indices changes upon disease, in particular malignancy, or treatment.

Appendix

Propagation of error

The error in estimating the true integrals of citrate ¹³C carbons found in ¹³C MR spectra results in an error in the estimation of proposed ratios R_1 and R_2 .

$$R_1 = \frac{C2/4 - C3}{C2/4} \quad (59)$$

$$R_1 \pm \sigma_{R_1} = \frac{(C2/4 \pm \sigma_{C2/4}) - (C3 \pm \sigma_{C3})}{(C2/4 \pm \sigma_{C2/4})} \quad (60)$$

$$(61)$$

We assume a similar error on all ^{13}C MR signals, so $\sigma_{C3} = \sigma_{C2/4} = \sigma$. This means the standard error can be estimated using the following equations:

$$\frac{\sigma_{R_1}}{R_1} \approx \sqrt{\frac{2\sigma^2}{(C2/4 - C3)^2} + \frac{\sigma^2}{C2/4^2}} \quad (62)$$

$$= \sqrt{\frac{2\sigma^2}{R_1^2 C2/4^2} + \frac{\sigma^2}{C2/4^2}} \quad (63)$$

$$= \frac{\sigma}{C2/4} \sqrt{\frac{2}{R_1^2} + 1} \quad (64)$$

This means that if we assume the standard error to be a fraction α of the largest integral, there are two possible solutions

$$\frac{\sigma_{R_1}}{R_1} \approx \alpha \sqrt{\frac{2}{R_1^2} + 1} \quad \text{for } C2/4 \geq C3, \sigma = \alpha C2/4 \quad (65)$$

$$\frac{\sigma_{R_1}}{R_1} \approx \alpha(1 - R_1) \sqrt{\frac{2}{R_1^2} + 1} \quad \text{for } C2/4 \leq C3, \sigma = \alpha C3 \quad (66)$$

For ratio R_2 a similar derivation can be used

$$R_2 = \frac{C1/5}{C3} \quad (67)$$

$$R_2 \pm \sigma_{R_2} = \frac{(C1/5 \pm \sigma_{C1/5})}{(C3 \pm \sigma_{C3})} \quad (68)$$

We assume a similar error on all ^{13}C MR signals, so $\sigma_{C3} = \sigma_{C1/5} = \sigma$. This means the standard error can be estimated using the following equations:

$$\frac{\sigma_{R_2}}{R_2} \approx \sqrt{\frac{\sigma^2}{C1/5^2} + \frac{\sigma^2}{C3^2}} \quad (69)$$

$$= \sqrt{\frac{\sigma^2}{R_2^2 C3^2} + \frac{\sigma^2}{C3^2}} \quad (70)$$

$$= \frac{\sigma}{C3} \sqrt{\frac{1}{R_2^2} + 1} \quad (71)$$

This means that if we assume again that the standard error is a fraction α of the largest integral, there are two possible solutions:

$$\frac{\sigma_{R_2}}{R_2} \approx \alpha \sqrt{\frac{1}{R_2^2} + 1} \quad \text{for } C3 \geq C1/5, \sigma = \alpha C3 \quad (72)$$

$$\frac{\sigma_{R_2}}{R_2} \approx \alpha \sqrt{1 + R_2^2} \quad \text{for } C3 \leq C1/5, \sigma = \alpha C1/5 \quad (73)$$

These equations are used in plotting the error bounds in Figure 12.

Average number of Krebs cycle turns for a ^{13}C label

The average number of Krebs cycle turns that a ^{13}C carbon completes before ending up in either citrate or carbon dioxide depends on the carbon position it starts out from at $n = 0$. For a ^{13}C carbon starting at citrate C2 or C3 the fraction of ^{13}C carbon ending up in citrate during Krebs cycle turn n is:

$$C_{2/3}^{Citr}(n = 0) = c \quad (74)$$

$$C_{2/3}^{Citr}(n = 1) = c(1 - c) \quad (75)$$

$$C_{2/3}^{Citr}(n \geq 2) = \frac{c(1 - c)^n}{2^{n-2}} \quad (76)$$

And the fractions of ^{13}C carbon ending up in carbon dioxide at cycle turn n is:

$$C_{2/3}^{CO_2}(n = 0) = 0 \quad (77)$$

$$C_{2/3}^{CO_2}(n = 1) = 0 \quad (78)$$

$$C_{2/3}^{CO_2}(n \geq 2) = \frac{(1 - c)^{n+1}}{2^{n-1}} \quad (79)$$

Multiplying this by the corresponding Krebs cycle turn index n and summing this over all possible values of n gives us the average number of Krebs cycle turns a ^{13}C carbon starting at C2 or C3 completes before ending up in citrate or carbon dioxide.

$$\langle n_{C2/3}^{Citr} \rangle = \sum_{n=0}^{n=\infty} n C_{2/3}^{Citr}(n) = c(1 - c) \left(1 + 2 \frac{(1 - c)(3 + c)}{(1 + c)^2} \right) \quad (80)$$

$$\langle n_{C2/3}^{CO_2} \rangle = \sum_{n=0}^{n=\infty} n C_{2/3}^{CO_2}(n) = \frac{(3 + c)(1 - c)^3}{(1 + c)^2} \quad (81)$$

We can do the same for citrate C1 and C4, this results in:

$$C_{1/4}^{Citr}(n = 0) = c \quad (82)$$

$$C_{1/4}^{Citr}(n = 1) = c(1 - c) \quad (83)$$

$$C_{1/4}^{Citr}(n \geq 2) = 0 \quad (84)$$

And the following contributions for cycle turn n for carbon dioxide:

$$C_{1/4}^{CO_2}(n = 0) = 0 \quad (85)$$

$$C_{1/4}^{CO_2}(n = 1) = (1 - c)^2 \quad (86)$$

$$C_{1/4}^{CO_2}(n \geq 2) = 0 \quad (87)$$

Again we can calculate the average number of cycle turns a ^{13}C carbon starting at citrate C1 or C4 completes before secretion in citrate or ending up in carbon dioxide.

$$\langle n_{C1/4}^{Citr} \rangle = \sum_{n=0}^{n=\infty} n C_{1/4}^{Citr}(n) = c(1 - c) \quad (88)$$

$$\langle n_{C1/4}^{CO_2} \rangle = \sum_{n=0}^{n=\infty} n C_{1/4}^{CO_2}(n) = (1 - c)^2 \quad (89)$$

Depending on the ^{13}C substrate that is used the ^{13}C carbons in citrate start at different positions at $n = 0$. For $[1,6-^{13}\text{C}_2]\text{glucose}$ or $[3-^{13}\text{C}]\text{pyruvate}$ ^{13}C carbon ends up at C2 via the PDC route and at C3 or C4 via the PC route. For $[2,5-^{13}\text{C}_2]\text{glucose}$ or $[2-^{13}\text{C}]\text{pyruvate}$ the ^{13}C carbons start at citrate C1 via PDC and at citrate C3 or C4 via PC. The result is that the true average number of Krebs cycle turns a ^{13}C carbon completes before ending up in citrate or carbon dioxide also depends on the value of f^{PC} . Calculating this for the $[1,6-^{13}\text{C}_2]\text{glucose}$ or $[3-^{13}\text{C}]\text{pyruvate}$ substrates:

$$\langle n_{glc-1,6}^{Citr} \rangle = \left(f^{PDC} + \frac{1}{2}f^{PC} \right) \langle n_{C2/3}^{Citr} \rangle + \frac{1}{2}f^{PC} \langle n_{C1/4}^{Citr} \rangle \quad (90)$$

$$= \left(f^{PDC} + \frac{1}{2}f^{PC} \right) c(1-c) \left(1 + 2\frac{(1-c)(3+c)}{(1+c)^2} \right) + f^{PC} \frac{c(1-c)}{2} \quad (91)$$

$$\langle n_{glc-1,6}^{CO_2} \rangle = \left(f^{PDC} + \frac{1}{2}f^{PC} \right) \langle n_{C2/3}^{CO_2} \rangle + \frac{1}{2}f^{PC} \langle n_{C1/4}^{CO_2} \rangle \quad (92)$$

$$= \left(f^{PDC} + \frac{1}{2}f^{PC} \right) \frac{(3+c)(1-c)^3}{(1+c)^2} + f^{PC} \frac{(1-c)^2}{2} \quad (93)$$

And for the $[2,5-^{13}\text{C}_2]\text{glucose}$ or $[2-^{13}\text{C}]\text{pyruvate}$ substrate

$$\langle n_{glc-1,6}^{Citr} \rangle = \frac{1}{2}f^{PC} \langle n_{C2/3}^{Citr} \rangle + \left(f^{PDC} + \frac{1}{2}f^{PC} \right) \langle n_{C1/4}^{Citr} \rangle \quad (94)$$

$$= \frac{1}{2}f^{PC} c(1-c) \left(1 + 2\frac{(1-c)(3+c)}{(1+c)^2} \right) + \left(f^{PDC} + \frac{1}{2}f^{PC} \right) c(1-c) \quad (95)$$

$$\langle n_{glc-1,6}^{CO_2} \rangle = \frac{1}{2}f^{PC} \langle n_{C2/3}^{CO_2} \rangle + \left(f^{PDC} + \frac{1}{2}f^{PC} \right) \langle n_{C1/4}^{CO_2} \rangle \quad (96)$$

$$= \frac{1}{2}f^{PC} \frac{(3+c)(1-c)^3}{(1+c)^2} + \left(f^{PDC} + \frac{1}{2}f^{PC} \right) (1-c)^2 \quad (97)$$

The average number of Krebs cycle turns a ^{13}C carbon completes before being secreted in citrate or carbon dioxide is plotted for $f^{PC} = 0.2$ in Figure 13. The longer a ^{13}C stays in the Krebs cycle, the bigger the fraction that will be secreted as carbon dioxide, but also as citrate, the figure shows this balance and the optima. Depending on which ^{13}C substrates are used and the pyruvate carboxylase fraction f^{PC} , the maximum of the citrate curves shifts. At this maximum a ^{13}C carbon stays in citrate the longest.

References

1. Costello, L. C. & Franklin, R. B. Citrate metabolism of normal and malignant prostate epithelial cells. *Urology* **50**, 3–12. ISSN: 0090-4295. <http://www.sciencedirect.com/science/article/pii/S0090429597001246> (July 1997).
2. Costello, L. C., Liu, Y., Zou, J. & Franklin, R. B. Evidence for a Zinc Uptake Transporter in Human Prostate Cancer Cells Which Is Regulated by Prolactin and Testosterone. *Journal of Biological Chemistry* **274**, 17499–17504. ISSN: 0021-9258. <http://www.jbc.org/content/274/25/17499> (June 1999).
3. Bertilsson, H. *et al.* Changes in gene transcription underlying the aberrant citrate and choline metabolism in human prostate cancer samples. *Clinical cancer research : an official journal of the American Association for Cancer Research* **18**, 3261–9. ISSN: 1078-0432. <http://clincancerres.aacrjournals.org/content/18/12/3261.long> (June 2012).

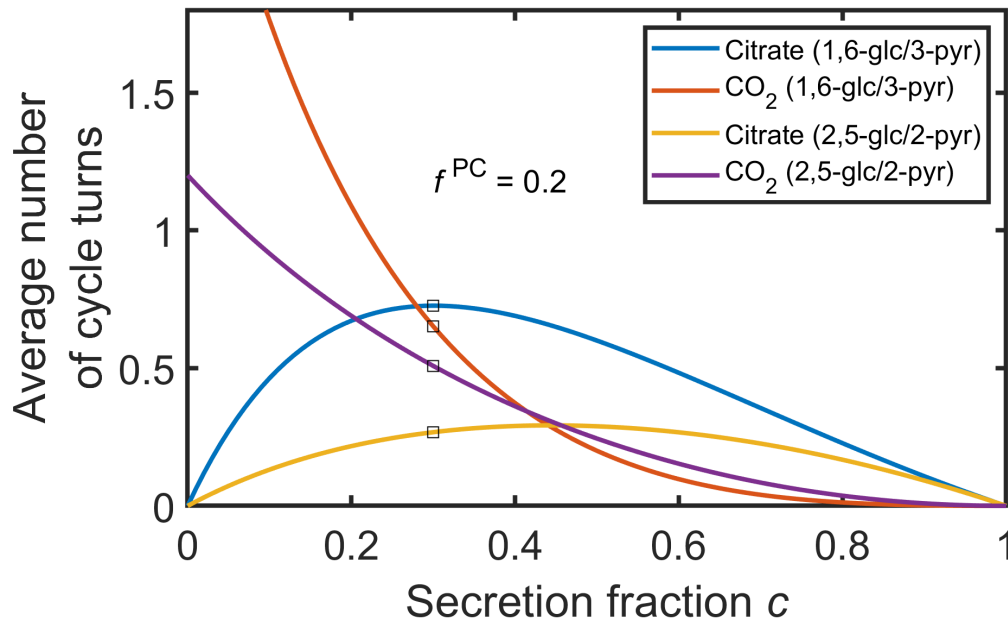


Figure 13: Average number of Krebs cycle turns a ^{13}C carbon completes before being secreted in citrate or being lost into carbon dioxide versus secretion fraction c . The fraction pyruvate carboxylase is set to $f^{PC} = 0.2$ and the values at $c = 0.3$ are indicated with squares.

4. Singh, K. K., Desouki, M. M., Franklin, R. B. & Costello, L. C. Mitochondrial aconitase and citrate metabolism in malignant and nonmalignant human prostate tissues. *Molecular Cancer* **5**, 14. ISSN: 14764598. <http://molecular-cancer.biomedcentral.com/articles/10.1186/1476-4598-5-14> (Apr. 2006).
5. Heerschap, A. *et al.* In vivo proton MR spectroscopy reveals altered metabolite content in malignant prostate tissue. *Anticancer research* **17**, 1455–60. ISSN: 0250-7005. <http://www.ncbi.nlm.nih.gov/pubmed/9179183>.
6. Kurhanewicz, J. *et al.* Citrate as an in vivo marker to discriminate prostate cancer from benign prostatic hyperplasia and normal prostate peripheral zone: Detection via localized proton spectroscopy. *Urology* **45**, 459–466. ISSN: 00904295. <http://www.ncbi.nlm.nih.gov/pubmed/7533458> <http://linkinghub.elsevier.com/retrieve/pii/S009042959800168> (Mar. 1995).
7. Kurhanewicz, J. & Vigneron, D. B. Magnetic Resonance Imaging and Spectroscopy of Prostate Cancer. *eMagRes* **5**, 923–944 (2016).
8. Bray, F., Ren, J.-S., Masuyer, E. & Ferlay, J. Global estimates of cancer prevalence for 27 sites in the adult population in 2008. *International Journal of Cancer* **132**, 1133–1145. ISSN: 00207136. <http://doi.wiley.com/10.1002/ijc.27711> (Mar. 2013).
9. Ferlay J, Soerjomataram I, Ervik M, Dikshit R, Eser S, Mathers C, Rebelo M, Parkin DM, Forman D, Bray F. *IARC CancerBase No. 11; Cancer Incidence and Mortality Worldwide* <http://globocan.iarc.fr>.

10. Kelly, R. S., Vander Heiden, M. G., Giovannucci, E. & Mucci, L. A. Metabolomic Biomarkers of Prostate Cancer: Prediction, Diagnosis, Progression, Prognosis, and Recurrence. *Cancer epidemiology, biomarkers & prevention : a publication of the American Association for Cancer Research, cosponsored by the American Society of Preventive Oncology* **25**, 887–906. ISSN: 1538-7755. <http://www.ncbi.nlm.nih.gov/pubmed/27197278> <http://www.pubmedcentral.nih.gov/articlerender.fcgi?artid=PMC4891222> (June 2016).
11. Tayari, N., Heerschap, A., Scheenen, T. W. & Kobus, T. In vivo MR spectroscopic imaging of the prostate, from application to interpretation. *Analytical Biochemistry* **529**, 158–170. ISSN: 0003-2697. <https://www.sciencedirect.com/science/article/pii/S000326971730060X?via%7B%5C%7D3Dihub> (July 2017).
12. Testa, C., Pultrone, C., Manners, D. N., Schiavina, R. & Lodi, R. Metabolic Imaging in Prostate Cancer: Where We Are. *Frontiers in Oncology* **6**, 225. ISSN: 2234-943X. <http://journal.frontiersin.org/article/10.3389/fonc.2016.00225/full> (Nov. 2016).
13. Twum-ampofo, J., Fu, D.-x., Passaniti, A., Hussain, A. & Siddiqui, M. M. Metabolic targets for potential prostate cancer therapeutics. *Current Opinion in Oncology* **28**, 241–247. ISSN: 1040-8746. <https://insights.ovid.com/pubmed?pmid=26907571> (May 2016).
14. Schmidt, K., Carlsen, M., Nielsen, J. & Villadsen, J. Modeling isotopomer distributions in biochemical networks using isotopomer mapping matrices. *Biotechnology and Bioengineering*. ISSN: 00063592 (1997).
15. Wiechert, W., Möllney, M., Isermann, N., Wurzel, M. & De Graaf, A. A. Bidirectional reaction steps in metabolic networks: III. Explicit solution and analysis of isotopomer labeling systems. *Biotechnology and Bioengineering*. ISSN: 00063592 (1999).
16. Antoniewicz, M. R., Kelleher, J. K. & Stephanopoulos, G. Elementary metabolite units (EMU): A novel framework for modeling isotopic distributions. *Metabolic Engineering* **9**, 68–86. ISSN: 10967176. arXiv: NIHMS150003. <https://www.sciencedirect.com/science/article/pii/S109671760600084X?via%7B%5C%7D3Dihub> (Jan. 2007).
17. Shestov, A. A. *et al.* Bonded Cumomer Analysis of Human Melanoma Metabolism Monitored by ¹³C NMR Spectroscopy of Perfused Tumor Cells. *Journal of Biological Chemistry* **291**, 5157–5171. ISSN: 0021-9258. <http://www.jbc.org/content/291/10/5157.long> <http://www.ncbi.nlm.nih.gov/pubmed/26703469> <http://www.pubmedcentral.nih.gov/articlerender.fcgi?artid=PMC4777850> (Mar. 2016).
18. Shestov, A. A. *et al.* ¹³C MRS and LC-MS Flux Analysis of Tumor Intermediary Metabolism. *Frontiers in Oncology* **6**, 135. ISSN: 2234-943X. <http://journal.frontiersin.org/Article/10.3389/fonc.2016.00135/abstract> (June 2016).
19. PORTAIS, J.-C., SCHUSTER, R., MERLE, M. & CANIONI, P. Metabolic flux determination in C6 glioma cells using carbon-13 distribution upon [1-¹³C]glucose incubation. *European Journal of Biochemistry* **217**, 457–468. ISSN: 0014-2956. <http://doi.wiley.com/10.1111/j.1432-1033.1993.tb18265.x> (Oct. 1993).
20. Wu, F., Yang, F., Vinnakota, K. C. & Beard, D. A. Computer modeling of mitochondrial tricarboxylic acid cycle, oxidative phosphorylation, metabolite transport, and electrophysiology. *The Journal of biological chemistry* **282**, 24525–37. ISSN: 0021-9258. <http://www.ncbi.nlm.nih.gov/pubmed/17591785> (Aug. 2007).

21. Jiang, L. *et al.* Quantitative metabolic flux analysis reveals an unconventional pathway of fatty acid synthesis in cancer cells deficient for the mitochondrial citrate transport protein. *Metabolic Engineering* **43**, 198–207. ISSN: 1096-7176. <https://www.sciencedirect.com/science/article/pii/S1096717616302166?via%7B%5C%7D3Dihub%7B%5C%7Ddbib11> (Sept. 2017).
22. Young, J. D., Walther, J. L., Antoniewicz, M. R., Yoo, H. & Stephanopoulos, G. An elementary metabolite unit (EMU) based method of isotopically nonstationary flux analysis. *Biotechnology and Bioengineering* **99**, 686–699. ISSN: 00063592. <http://doi.wiley.com/10.1002/bit.21632> (Feb. 2008).
23. Egnatchik, R. A. *et al.* Glutamate-oxaloacetate transaminase activity promotes palmitate lipotoxicity in rat hepatocytes by enhancing anaplerosis and citric acid cycle flux. *The Journal of biological chemistry*, jbc.RA118.004869. ISSN: 1083-351X. <http://www.ncbi.nlm.nih.gov/pubmed/30563841> (Dec. 2018).
24. Xin, L., Lanz, B., Lei, H. & Gruetter, R. Assessment of metabolic fluxes in the mouse brain in vivo using ^1H - ^{13}C NMR spectroscopy at 14.1 Tesla. *Journal of Cerebral Blood Flow and Metabolism* **35**, 759–765. ISSN: 15597016. <http://journals.sagepub.com/doi/10.1038/jcbfm.2014.251> (May 2015).
25. Carvalho, R. A. *et al.* A ^{13}C isotopomer kinetic analysis of cardiac metabolism: influence of altered cytosolic redox and $[\text{Ca}^{2+}]_i$. *American Journal of Physiology-Heart and Circulatory Physiology* **287**, H889–H895. ISSN: 0363-6135. <http://www.physiology.org/doi/10.1152/ajpheart.00976.2003> (Aug. 2004).
26. Malloy, C. R., Jones, J. G., Jeffrey, F. M., Jessen, M. E. & Sherry, A. D. Contribution of various substrates to total citric acid cycle flux and anaplerosis as determined by ^{13}C isotopomer analysis and O_2 consumption in the heart. *MAGMA Magnetic Resonance Materials in Physics, Biology, and Medicine* **4**, 35–46. ISSN: 0968-5243. <http://link.springer.com/10.1007/BF01759778> (Mar. 1996).
27. Burgess, S. C., Babcock, E. E., Jeffrey, F. H., Sherry, A. & Malloy, C. R. NMR indirect detection of glutamate to measure citric acid cycle flux in the isolated perfused mouse heart. *FEBS Letters* **505**, 163–167. ISSN: 0014-5793. <https://www.sciencedirect.com/science/article/pii/S0014579301027995> (Sept. 2001).
28. Yang, J. & Shen, J. Increased oxygen consumption in the somatosensory cortex of α -chloralose anesthetized rats during forepaw stimulation determined using MRS at 11.7 Tesla. *NeuroImage* **32**, 1317–1325. ISSN: 1053-8119. <https://www.sciencedirect.com/science/article/pii/S1053811906005763?via%7B%5C%7D3Dihub%7B%5C%7Ddbib8> (Sept. 2006).
29. Chen, W. *et al.* Study of tricarboxylic acid cycle flux changes in human visual cortex during hemifield visual stimulation using ^1H - $\{^{13}\text{C}\}$ MRS and fMRI. *Magnetic Resonance in Medicine* **45**, 349–355. ISSN: 0740-3194. <http://doi.wiley.com/10.1002/1522-2594%7B%5C%7D28200103%7B%5C%7D2945%7B%5C%7D3A3%7B%5C%7D3C349%7B%5C%7D3A%7B%5C%7D3AAID-MRM1045%7B%5C%7D3E3.O.CO%7B%5C%7D3B2-8> (Mar. 2001).
30. Mason, G. F. *et al.* Simultaneous Determination of the Rates of the TCA Cycle, Glucose Utilization, α -Ketoglutarate / Glutamate Exchange, and Glutamine Synthesis in Human Brain by NMR. *Journal of Cerebral Blood Flow & Metabolism* **15**, 12–25. ISSN: 0271-678X. <http://journals.sagepub.com/doi/10.1038/jcbfm.1995.2> (Jan. 1995).
31. Cheshkov, S. *et al.* Oxidation of $[\text{U-}^{13}\text{C}]$ glucose in the human brain at 7T under steady state conditions. *Magnetic Resonance in Medicine* **78**, 2065–2071. ISSN: 15222594. <http://doi.wiley.com/10.1002/mrm.26603> (Dec. 2017).

32. Owen, O. E., Kalhan, S. C. & Hanson, R. W. The key role of anaplerosis and cataplerosis for citric acid cycle function. *The Journal of biological chemistry* **277**, 30409–12. ISSN: 0021-9258. <http://www.ncbi.nlm.nih.gov/pubmed/12087111> (Aug. 2002).
33. Chen, H.-Y. *et al.* Assessing Prostate Cancer Aggressiveness with Hyperpolarized Dual-Agent 3D Dynamic Imaging of Metabolism and Perfusion. *Cancer research* **77**, 3207–3216. ISSN: 1538-7445. <http://www.ncbi.nlm.nih.gov/pubmed/28428273><http://www.pubmedcentral.nih.gov/articlerender.fcgi?artid=PMC5484421> (June 2017).
34. Bancroft Brown, J. *et al.* NMR quantification of lactate production and efflux and glutamate fractional enrichment in living human prostate biopsies cultured with [1,6-¹³C₂]glucose. *Magnetic Resonance in Medicine* **82**, 566–576. ISSN: 0740-3194. <https://onlinelibrary.wiley.com/doi/abs/10.1002/mrm.27739> (Aug. 2019).
35. Cornel, E. B. *et al.* In vitro proton magnetic resonance spectroscopy of four human prostate cancer cell lines. *The Prostate* **26**, 275–80. ISSN: 0270-4137. <http://www.ncbi.nlm.nih.gov/pubmed/7753713> (May 1995).
36. Franklin, R. B., Juang, H. H., Zou, J. & Costello, L. C. Regulation of citrate metabolism by androgen in the LNCaP human prostate carcinoma cell line. *Endocrine* **3**, 603–7. ISSN: 1355-008X. <http://www.ncbi.nlm.nih.gov/pubmed/21153139> (Aug. 1995).
37. Korenchuk, S. *et al.* VCaP, a cell-based model system of human prostate cancer. *In vivo (Athens, Greece)* **15**, 163–8. ISSN: 0258-851X. <http://www.ncbi.nlm.nih.gov/pubmed/11317522>.
38. Vanhamme, L., van den Boogaart, A. & Van Huffel, S. Improved Method for Accurate and Efficient Quantification of MRS Data with Use of Prior Knowledge. *Journal of Magnetic Resonance* **129**, 35–43. ISSN: 1090-7807. <https://www.sciencedirect.com/science/article/pii/S1090780797912441?via%7B%5C%7D3Dihub> (Nov. 1997).
39. Naressi, A. *et al.* Java-based graphical user interface for the MRUI quantitation package. *Magma: Magnetic Resonance Materials in Physics, Biology, and Medicine* **12**, 141–152. ISSN: 1352-8661. <http://link.springer.com/10.1007/BF02668096> (June 2001).
40. Stefan, D. *et al.* Quantitation of magnetic resonance spectroscopy signals: the jMRUI software package. *Measurement Science and Technology* **20**, 104035. ISSN: 0957-0233. <http://stacks.iop.org/0957-0233/20/i=10/a=104035?key=crossref.d6dc8615cb88426675ce9638bb30b723> (Oct. 2009).
41. Magnusson, I. *et al.* Noninvasive tracing of Krebs cycle metabolism in liver. *Journal of Biological Chemistry* **266**, 6975–6984. ISSN: 00219258 (1991).
42. Merritt, M. E., Harrison, C., Sherry, A. D., Malloy, C. R. & Burgess, S. C. Flux through hepatic pyruvate carboxylase and phosphoenolpyruvate carboxykinase detected by hyperpolarized ¹³C magnetic resonance. *Proceedings of the National Academy of Sciences of the United States of America* **108**, 19084–19089. ISSN: 00278424 (2011).